

# 3-((R)-4-(((R)-6-(2-Bromo-4-fluorophenyl)-5-(ethoxycarbonyl)-2-(thiazol-2-yl)-3,6-dihydropyrimidin-4-yl)methyl)morpholin-2-yl)propanoic Acid (HEC72702), a Novel Hepatitis B Virus Capsid Inhibitor Based on Clinical Candidate GLS4

Qingyun Ren,<sup>\*,†,‡,§</sup> Xinchang Liu,<sup>†,‡</sup> Guanghua Yan,<sup>†,‡</sup> Biao Nie,<sup>†</sup> Zhifu Zou,<sup>†,‡</sup> Jing Li,<sup>†</sup> Yunfu Chen,<sup>†</sup> Yu Wei,<sup>†</sup> Jianzhou Huang,<sup>†,‡</sup> Zhonghua Luo,<sup>†</sup> Baohua Gu,<sup>†</sup> Siegfried Goldmann,<sup>†,‡,§</sup> Jiancun Zhang,<sup>§</sup> and Yingjun Zhang<sup>\*,†</sup>

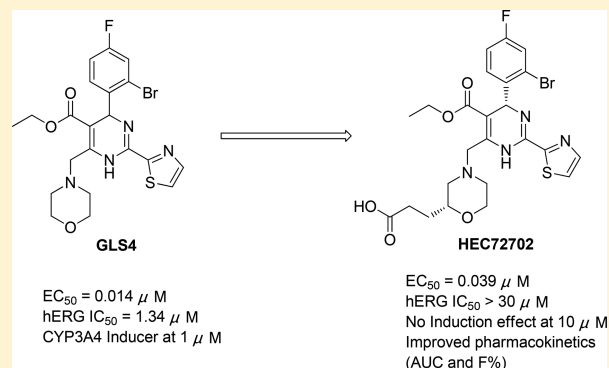
<sup>†</sup>The State Key Laboratory of Anti-Infection Drug Development, HEC Pharma Group, Dong Guan 523871, China

<sup>‡</sup>Anti-infection Innovation Department, New Drug Research Institute, HEC Pharma Group, Dong Guan 523871, China

<sup>§</sup>Guangzhou Institute of Biomedicine and Health, Chinese Academy of Sciences, Guangzhou 510530, China

## Supporting Information

**ABSTRACT:** The inhibition of hepatitis B virus (HBV) capsid assembly is a novel strategy for the development of chronic hepatitis B (CHB) therapeutics. On the basis of the preclinical properties and clinical results of GLS4, we carried out further investigation to seek a better candidate compound with appropriate anti-HBV potency, reduced hERG activity, decreased CYP enzyme induction, and improved pharmacokinetic (PK) properties. To this end, we have successfully found that morpholine carboxyl analogues with comparable anti-HBV activities to that of GLS4 showed decreased hERG activities, but they displayed strong CYP3A4 induction in a concentration-dependent manner, except for morpholine propionic acid analogues. After several rounds of modification, compound **58** (HEC72702), which had an (R)-morpholine-2-propionic acid at the C6 position of its dihydropyrimidine core ring, was found to display no induction of the CYP1A2, CYP3A4, or CYP2B6 enzyme at the high concentration of 10  $\mu$ M. In particular, it demonstrated a good systemic exposure and high oral bioavailability and achieved a viral-load reduction greater than 2 log in a hydrodynamic-injected (HDI) HBV mouse model and has now been selected for further development.



## INTRODUCTION

HBV infection is a serious global public-health problem, with more than 350 million people, especially in Asia-Pacific regions, chronically infected by this small enveloped DNA virus. The disease progression for many of the infected persons will finally develop into more life-threatening diseases, such as liver failure, cirrhosis, or hepatocellular carcinomas (HCC).<sup>1,2</sup> It has been estimated that HBV infections directly or indirectly account for the deaths of 600 000 patients annually. Current treatment regimens rely mainly on the use of interferon- $\alpha$  (IFN) and nucleoside- or nucleotide-based reverse-transcriptase inhibitors. However, the clinical use of IFN and peg-IFN is limited by their low response rates (20–30%) among CHB patients and a slew of side effects, such as flu-like symptoms, anemia, leucopenia, thrombocytopenia, anorexia, and depression.<sup>3</sup> A major drawback of the nucleotide analogues is the emergence of drug resistance during long-term treatment, with approximately 70% of patients becoming resistant to lamivudine;<sup>4</sup> resistance to entecavir also occurs among lamivudine-pretreated patients at a rate of 43% after 4 years.<sup>5</sup> In order to improve the

treatment of CHB and reduce drug resistance, the development of novel agents with different therapeutic targets besides viral polymerase is highly necessary.<sup>6</sup>

The HBV capsid plays indispensable roles in viral DNA synthesis from the pregenome and in intracellular trafficking. HBV persistence and transmission require HBV replication, which depends on the assembly of a nucleocapsid composed of capsid proteins, reverse transcriptase, and pregenomic RNA.<sup>7</sup> Furthermore, the encapsidation of HBV pregenomic RNA (pgRNA) is an evolutionarily constrained process,<sup>8</sup> and this genetic stability makes HBV-capsid formation a better drug target against various genotypes of HBV polymerase-resistant mutants.<sup>9</sup>

Some phenylpropenamide derivatives, such as **1** (AT-61), **2** (AT-130),<sup>10,11</sup> the sulfamoylbenzamide **3** (DVR23),<sup>12</sup> and **4** (isothiafludine),<sup>13</sup> shown in Figure 1, have been shown to inhibit pgRNA packaging, which leads to the formation of

Received: December 28, 2017

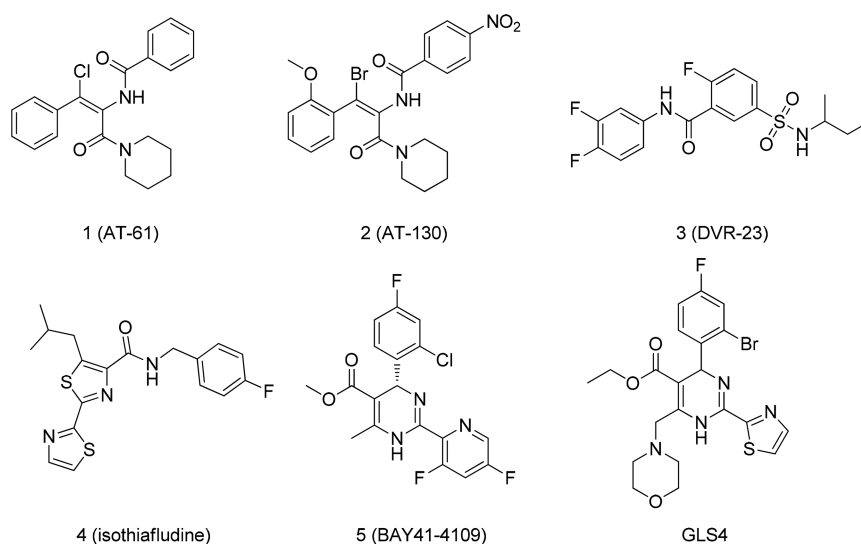


**Figure 1.** Chemical structures of the reported HBV-capsid inhibitors.

pgRNA-free empty capsids. These agents were found to be potent against HBV replication in various human hepatoma cell lines. Among them, NVR-3778 (unreported structure), a sulfamoylbenzamide compound, has progressed into phase I, and the clinical-phase Ib results show that at a dosage of 600 mg twice daily (b.i.d.), this compound could reduce serum HBV-DNA levels to 1.72 log 10.<sup>14</sup> Jassen has also completed the phase I clinical trials of JNJ-379 (unreported structure), which is reported to possess the same mechanism as NVR-3778 but with improved efficacy and a better safety profile.<sup>15</sup>

Bay 41-4109 (**5**, Figure 1) has been reported to disrupt or misdirect the assembly of the HBV capsid, which leads to capsid depletion and then termination of the viral replication process.<sup>16,17</sup> Bay 41-4109 was shown to prevent HBV infections in a transgenic HBV model by reducing HBV viral DNA in the liver and plasma, but it was found to be hepatotoxic at high doses in rats; thus, the follow-up studies of this compound were suspended.<sup>18,19</sup> A currently reported compound in clinical stage I with a similar mechanism as Bay 41-4109 was RG7689 (unreported structure), and preclinical experiments of this compound showed that it could suppress viral replication continually and prevent the formation of new cccDNA.<sup>20,21</sup>

GLS4 (Figure 1) also possesses the same mechanism as BAY41-4109, having been developed as a capsid inhibitor, and is currently in the phase II clinical stage. The preclinical anti-HBV efficacy, mechanism of action, and pharmacological properties of GLS4 have been recently published in several articles.<sup>22–25</sup> It was reported that GLS4 demonstrated potent inhibitory activities against wild and various drug-resistant HBV strains in a HepG2-cell-transfection assay. However, it was found that GLS4 alone could not achieve anticipated blood concentrations to show the desired antiviral effect in phase I clinical trials, which likely resulted from its fast metabolism and moderate induction of the CYP3A4 enzyme (see Table 3). To address this problem, a combination of GLS4 and ritonavir (RTV) was used in the ensuing clinical trials. This approach proved to be successful, with significant increases in the plasma concentrations in the healthy volunteers and substantial decreases in HBV-DNA levels in CHB patients.

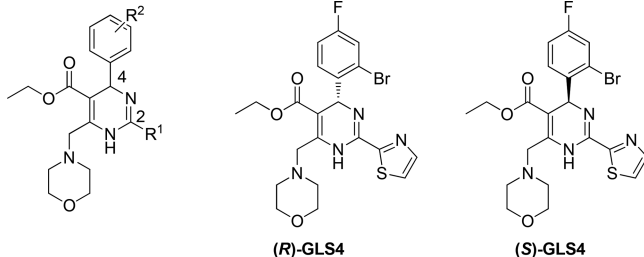
Some drugs have been withdrawn from the market because of prolonged QT intervals due to hERG inhibition.<sup>26,27</sup> At first glance, GLS4 might cause some concerns of a QT-prolongation

risk, because of its moderate inhibition of the hERG channel (hERG IC<sub>50</sub> = 1.34 μM, Table 1). However, after careful reasoning and assessment, we believe that GLS4 should be safe enough for humans because of following results: (i) the safety window of GLS4 is large enough (hERG IC<sub>50</sub>/EC<sub>50</sub> > 1000), (ii) no cardiac toxicity is associated with hERG in 6 month repeated toxicity tests with mice and 9 month repeated toxicity tests with beagle dogs, and (iii) no obvious side effects have been observed so far from monitoring cardiac-toxicity-associated indicators (QT durations) in clinical trials. In conclusion, GLS4 was found to be safe enough in clinical trials, and continuing clinical trials are currently underway. However, having the potential safety risk of the use of GLS4 in the long-term treatment of HBV patients in mind, we aimed to search for a second-generation backup compound for GLS4. Thus, we set out with the goal of finding a backup compound for GLS4 with the appropriate anti-HBV potency, significantly reduced hERG activity, decreased induction of the CYP enzyme, and improved pharmacokinetic (PK) properties. Herein, we report the discovery of compound **58**, which appeared to be free of all the drawbacks associated with GLS4 and has been selected for further development as an oral anti-HBV-infection agent.

## RESULTS AND DISCUSSION

**Structure and hERG Activity.** To ameliorate the hERG inhibition of GLS4, we started to search for a backup compound for GLS4. We set to design and synthesize new derivatives with reduced or diminished hERG activity. Common approaches to decrease hERG activity include structural modifications, formation of zwitterions, control of lipophilicity, and attenuation of the pK<sub>a</sub> of the molecule.<sup>28</sup> To this end, we first separated the racemate of GLS4 and found that the *R* and *S* enantiomers showed no difference in their hERG activities (Table 1). Then, we replaced the dihydropyrimidine core with triazine and several other fused heterocycles to give compounds **6–9**. The dihydropyrimidine core was oxidized to give pyrimidine compound **10**, and N-alkylation with a hydrophilic hydroxyethyl halide gave compound **11**. As shown in Figure 2, although these compounds displayed decreased hERG inhibitions (for compound **10**, hERG IC<sub>50</sub> > 10 μM), they also exhibited dramatic drops in their anti-HBV activities (EC<sub>50</sub> > 16.4 μM). Thus, we started to modify the

Table 1. Anti-HBV Activities and hERG Activities of Molecules Generated via C2 and C4 Modifications



Compds	R <sup>1</sup>	R <sup>2</sup>	EC <sub>50</sub> <sup>a</sup> ( $\mu$ M)	hERG IC <sub>50</sub> <sup>b</sup> ( $\mu$ M)	Compds	R <sup>1</sup>	R <sup>2</sup>	EC <sub>50</sub> <sup>a</sup> ( $\mu$ M)	hERG IC <sub>50</sub> <sup>b</sup> ( $\mu$ M)
GLS4		2-Br-4-F	0.013	1.34	17		2-Br-4-F	0.035	3.49
GLS4JHS		2-Br-4-F	0.016	0.86	18		2-Br-4-F	0.069	0.90
(R)-GLS4		2-Br-4-F	0.0098	4.50	19		2-Br-4-F	0.042	3.80
(S)-GLS4		2-Br-4-F	3.367	4.88	20		2-Br-4-F	0.015	0.17
12		2-Cl-4-F	0.005	2.31	21		2-Br-4-F	>16.4	0.7
13		2-Cl-4-Cl	0.003	0.30	22		2-Br-4-F	>16.4	>10
14		2-Cl	0.016	4.04	23		2-Br-4-F	>16.4	4.19
15		2-NO <sub>2</sub>	0.1	0.26	24		2-Br-4-F	0.107	1.64
16		2-Ph-4-F	>16.4	4.96	25		2-Br-4-F	>16.4	>10

<sup>a</sup>EC<sub>50</sub> represents the mean values for the reduction of HBV-DNA levels by 50% in HepG.2.2.15 cells. Experiments were done in duplicate with variations of <15%. <sup>b</sup>hERG IC<sub>50</sub> represents the mean values for the 50% inhibition of hERG in CHO cells ( $N = 3$ ). Cisapride was used as a positive control, and the maximum concentration used was 10  $\mu$ M. IC<sub>50</sub> > 10  $\mu$ M is reported if the inhibition at 10  $\mu$ M is lower than 50%.

peripheral substituents while keeping the dihydropyrimidine core ring unchanged.

Our previous studies indicated that the ester group at the C5 position of GLS4 (see structure of GLS4 for the numbering convention) contacted a limited hydrophobic pocket so that polar and large groups were generally not tolerated.<sup>29</sup> After investigating various ester substitutions at the C5 position, we found that only the methyl ester and ethyl ester were well tolerated. We therefore decided to focus on conducting further modifications at the C2, C4, and C6 positions of the core dihydropyrimidine structure to improve or retain anti-HBV activity while decreasing hERG-inhibitory activity. The reported cocrystal structure (PDB ID 2G34)<sup>30</sup> indicated that the C4 position of the core dihydropyrimidine was located in a conserved and large hydrophobic pocket, and we also found that bulky groups, such as biphenyl groups, and hydrophilic substituents, such as carboxyl groups, were not tolerated.<sup>29</sup>

Thus, we made some small changes on the substituents at the C4 phenyl and found that these changes had no significant effect on anti-HBV activity (GLS4, 12, 13, and 14; Table 1). These compounds, however, showed no obvious improvement in their hERG activities. It was also observed that the hERG activities of these compounds increased with increasing cLogP. The order of the hERG activities of compounds GLS4 to 14 was as follows: 13 (hERG IC<sub>50</sub> = 0.30  $\mu$ M, cLogP = 5.17) > GLS4 (hERG IC<sub>50</sub> = 1.34  $\mu$ M, cLogP = 4.75) > 12 (hERG IC<sub>50</sub> = 2.31  $\mu$ M, cLogP = 4.60) > 14 (hERG IC<sub>50</sub> = 4.04  $\mu$ M, cLogP = 4.45). Replacement of the 2-bromine atom on the 4-phenyl group in GLS4 with NO<sub>2</sub> or phenyl gave compounds 15 and 16, but these two compounds were less active against HBV than GLS4, and their hERG activities showed no obvious improvements.

Next, we investigated the modification at the C2 position. Replacing the C2 thiazolyl with thiazolyl and thiophenyl

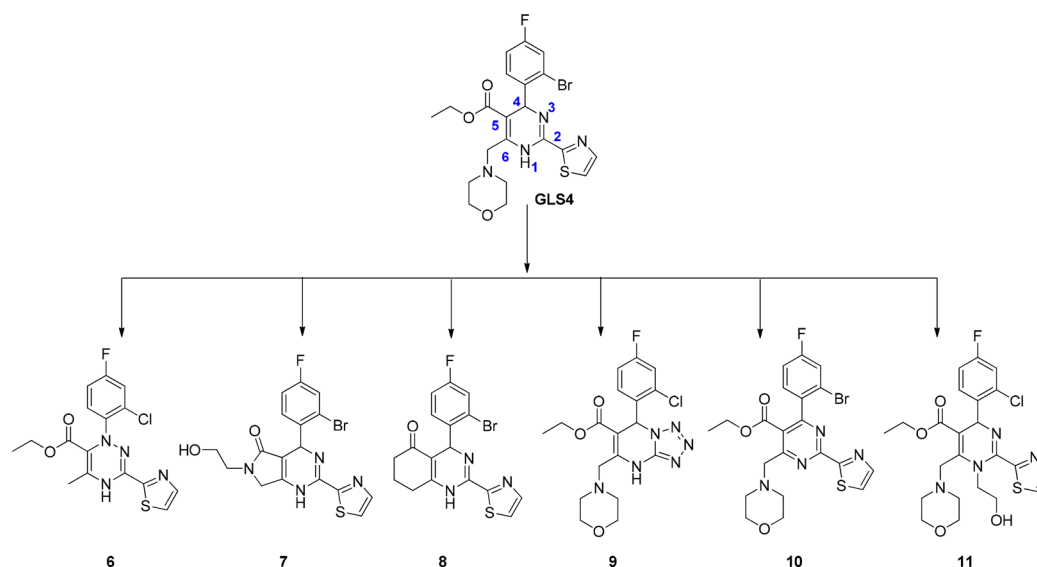


**Figure 2.** Previous design structure of molecules from GLS4.

resulted in compounds **17** and **18**, respectively. These two compounds showed similar anti-HBV activities to each other but decreased activities in comparison with GLS4. In the hERG-activity studies, compound **17** showed decreased hERG inhibition ( $IC_{50} = 3.49 \mu M$ ), whereas compound **18** showed increased hERG activity ( $IC_{50} = 0.9 \mu M$ ). Apparently, lipophilicity was a key determinant for the cLogP of the 2-thiophenyl compound, **18**, being much higher than that of compound **17** (cLogP = 6.05 vs 3.66). Further replacement of the thiazolyl group in GLS4 with pyridine, *N*-methyl-imidazole, triazole, and substituted thiazole led to compounds **19**, **20**, **21**, **23**, and **24**, but none of these compounds showed obvious improvements in hERG inhibition. However, we found that modification with a tetrazole at the C2 position (compound **22**) showed decreased hERG activity ( $IC_{50} > 10 \mu M$ ) but at the expense of decreased anti-HBV activity ( $EC_{50} > 16.4 \mu M$ ). The 3-methyl acetate of thiazole **24** was hydrolyzed to carboxylic acid to give compound **25**, which showed decreased hERG activity ( $IC_{50} > 10 \mu M$ ), but this compound also lost the anti-HBV activity. On the basis of the above results, we believed that it would be difficult to obtain compounds with optimal anti-HBV activities and low hERG activities when the structure modifications were made on the C2 and C4 positions of dihydropyrimidine, and importantly, it seemed possible to reduce hERG activity when a hydrophilic group, such as carboxylic acid or tetrazole, was introduced.

On the basis of the preliminary SARs at the C2 and C4 positions, we decided to introduce less lipophilic or hydrophilic groups to the C6 position by replacing the morpholine moiety of GLS4 (Table 2). First, the substitution of the morpholine group with thiomorpholine monoxide or dioxide led to compounds **26** and **27** whose anti-HBV activities were about 10 times less than that of GLS4. The more hydrophilic thiomorpholine monoxide, **26**, showed less hERG inhibition than thiomorpholine dioxide, **27**. It was further confirmed that the hERG activity could be adjusted by lipophilicity, and thus some hydrophilic groups, such as phenylalanine and proline, were introduced. The resultant compounds, **28** and **29**, exhibited moderate anti-HBV activities and lower hERG activities. The common "bioisosteres" of proline, piperidine carboxylic acid and piperazine carboxylic acid, on the C6

position led to compounds **30** and **31**, which showed decreased hERG inhibitions and lower anti-HBV activities. It seemed reasonable that compounds **30** and **31** showed decreased anti-HBV activities because a polar carboxylic acid substituent was not tolerated in the large hydrophobic binding pocket located at the interface of the capsid dimers. However, to our delight, the introduction of various morpholine carboxyl groups at the C6 position, affording compounds **32**, **33**, and **34**, resulted in comparable anti-HBV activities to that of GLS4 and lower hERG inhibitions (hERG  $IC_{50} > 10 \mu M$ ). Moreover, an additional methyl group, as in compound **35** ( $EC_{50} = 0.0093 \mu M$ ), resulted in a 5-fold higher potency than that of **32** ( $EC_{50} = 0.043 \mu M$ ). In contrast, the dimethyl morpholine carboxylic acid analogue, **36**, demonstrated reduced anti-HBV activity ( $EC_{50} = 3.924 \mu M$ ), suggesting that the substituent position of the methyl was important.

Further derivatization of the carboxylic acid of **32** gave rise to esters **37** and **38**, carboxamides **39** and **40**, sulfonamide **41**, and alcohols **42** and **43**, and all of these compounds maintained low hERG activities. Among them, **37**, **38**, **39**, **42**, and **43** showed increased or comparable anti-HBV potencies to that of GLS4. Large substitutions on the morpholine carboxyls of the ester and carboxamide were did not result in good anti-HBV activities, as in **40** and **41**. Although the ester **37** and the carboxamide **39** displayed favorable increases in anti-HBV activities and significantly decreased hERG activities as compared with those of **32** and GLS4, further development of these compounds (**37**–**43**) was not continued because of their high liver-microsome clearances (data not shown). Further studies revealed that both the substitution position and chain length of the carboxyl group were crucial for anti-HBV activity. The corresponding morpholine-2-carboxyl analogue, **44**, was much less active than **32**, and the extended acetic acid analogues, **45** and **46**, also showed reduced anti-HBV activities. In addition, to our surprise, the extended propanoic acid analogues, **47** and **48**, showed comparable anti-HBV activities to that of **32** and decreased hERG activities (hERG  $IC_{50} > 10 \mu M$ ).

To further investigate the relationship between anti-HBV activity and hERG activity, a series of compounds with good anti-HBV activities and low hERG activities in Table 2 were

Table 2. Anti-HBV Activities and hERG Activities of Molecules Generated via C6 Modifications

Comps	R <sup>2</sup>	R <sup>4</sup>	EC <sub>50</sub> <sup>a</sup> (μM)	hERG IC <sub>50</sub> <sup>b</sup> (μM)	Comps	R <sup>2</sup>	R <sup>4</sup>	EC <sub>50</sub> <sup>a</sup> (μM)	hERG IC <sub>50</sub> <sup>b</sup> (μM)
GLS4	2-Br-4-F		0.013	1.34	37	2-Br-4-F		0.011	>10
26	2-Br-4-F		0.1	5.74	38	2-Br-4-F		0.043	>10
27	2-Br-4-F		0.12	1.07	39	2-Br-4-F		0.011	>10
28	2-Br-4-F		0.486	8.68	40	2-Br-4-F		0.166	>10
29	2-Br-4-F		3.873	>10	41	2-Br-4-F		2.3	>10
30	2-Br-4-F		3.980	>10	42	2-Cl-4-Cl		0.036	>10
31	2-Br-4-F		>16.4	>10	43	2-Br-4-F		0.037	7.33
32	2-Br-4-F		0.043	>10	44	2-Br-4-F		2.37	>10
33	2-Cl-4-F		0.062	>10	45	2-Br-4-F		0.263	>10
34	2-Cl-4-Cl		0.028	>10	46	2-Br-4-F		0.499	>10
35	2-Br-4-F		0.0093	>10	47	2-Br-4-F		0.054	>10
36	2-Br-4-F		3.924	>10	48	2-Br-4-F		0.072	>10

<sup>a,b</sup>The definitions of EC<sub>50</sub> and hERG IC<sub>50</sub> are the same as those described in Table 1.

selected for chiral separation to obtain the chiral isomers to be screened.

All compounds with carboxyl groups in Table 3 showed no hERG inhibition at concentrations as high as 30 μM, except compound 54, which bore an alcohol group and showed an hERG IC<sub>50</sub> of 24.2 μM. These data further reveal the essential role of carboxyl groups in reducing the hERG activities of the analogues of GLS4.

Chirality is important for anti-HBV activity. It was found that the C4 *R*-configuration analogues have better anti-HBV activities than their corresponding C4 *S*-isomers. For example, without changing the C6 substituent, (*S*)-morpholine-3-carboxylic acid, the C4 *R*-configuration of compound 49,

(*R*)-49, showed the most potent anti-HBV activity, which was almost 400-fold more potent than that of the C4 *S*-isomer, (*S*)-49 (0.0057 vs 2.432 μM). This was in accordance with the result that (*R*)-GLS4 also showed 400-fold greater potency than (*S*)-GLS4 (0.0098 vs 3.367 μM). In addition, we further confirmed that the (*S*)-morpholine-3-carboxylic acid analogue demonstrated better anti-HBV activity than the corresponding (*R*)-morpholine-3-carboxylic acid analogue. For example, the (*S*)-morpholine-3-carboxylic acid analogue, (*R*)-49, showed nearly 50-fold greater potency than the corresponding (*R*)-morpholine-3-carboxylic acid analogue, (*R*)-50 (0.0057 vs 0.292 μM).

Table 3. Anti-HBV Activities and hERG Activities of Selected Chiral Isomers

Compds	R <sup>2</sup>	R <sup>4</sup>	EC <sub>50</sub> <sup>a</sup> (μM)	hERG IC <sub>50</sub> <sup>b</sup> (μM)	Compds	R <sup>5</sup>	EC <sub>50</sub> <sup>a</sup> (μM)	hERG IC <sub>50</sub> <sup>b</sup> (μM)
<b>49</b>	2-Cl-4-Cl		0.0086	>30	<b>(R)-53</b>		0.010	>30
<b>(R)-49</b>	2-Cl-4-Cl		0.0057	>30	<b>54</b>		0.021	24.2
<b>(S)-49</b>	2-Cl-4-Cl		2.432	>30	<b>55</b>		0.005	>30
<b>(R)-50</b>	2-Cl-4-Cl		0.292	>30	<b>56</b>		0.914	>30
<b>(S)-50</b>	2-Cl-4-Cl		>16.4	>30	<b>57</b>		0.005	>30
<b>51</b>	2-Cl-4-F		0.024	>30	<b>58</b>		0.039	>30
<b>52</b>	2-Cl-4-F		0.047	>30	<b>59</b>		0.094	>30
<b>(R)-52</b>	2-Cl-4-F		0.0048	>30	<b>60</b>		0.008	>30
<b>53</b>	2-Br-4-F		0.019	>30	<b>61</b>		0.154	>30

<sup>a</sup>The definition of EC<sub>50</sub> is the same as that described in Table 1. <sup>b</sup>hERG IC<sub>50</sub> represents the mean values for the 50% inhibition of hERG in HEK-293 cells (*N* = 3). Quinidine is used as a positive control, and the maximum compound concentration used is 30 μM. IC<sub>50</sub> > 30 μM is reported if the inhibition at 30 μM is lower than 50%.

Substitutions on the C4 phenyl ring affect activity, and the following order of anti-HBV activity was found: 2-Cl-4-Cl (**49**, EC<sub>50</sub> = 0.0086 μM) > 2-Br-4-F (**53**, EC<sub>50</sub> = 0.019 μM) > 2-Cl-4-F (**51**, EC<sub>50</sub> = 0.024 μM), which is in agreement with earlier modification trend (such as GLS4 and compounds **12** and **13** in Table 1). In addition, compounds with ethyl esters at the 5-position of dihydropyrimidine demonstrated about 2-fold higher potencies than compounds with methyl esters, as with compounds **51** and **52** (0.024 vs 0.047 μM). After chiral separation, the *R*-enantiomer of (**R**)-**53** showed a nearly 2-fold greater potency than racemic compound **53** (0.01 vs 0.019 μM), and the same situation occurred with (**R**)-**49** than **49** (0.0057 vs 0.0086 μM). An additional methyl introduction near the morpholine carboxyl group of (**R**)-**53** (EC<sub>50</sub> = 0.01 μM) led to **55**, which also showed a 2-fold improvement with an EC<sub>50</sub> of 0.005 μM. With a gem-dimethyl substituent on the other side of morpholine carboxyl, as in (**R**)-**53**, the anti-HBV potency was dramatically decreased, as compound **56** had an EC<sub>50</sub> of 0.914 μM. The 4,4-difluoroproline carboxyl analogue, **57**, was highly active, with an EC<sub>50</sub> of 0.005 μM, a potency comparable

to those of (**R**)-**52** and **55**. The substitution position of the propionic acid on morpholine had no consistent influence on anti-HBV activity, as compound **58** showed reduced activity compared with **60**, whereas **59** showed increased activity compared with **61**. Additionally, the influence of the absolute configuration of a propionic acid group on anti-HBV activity was studied in compounds **59** versus **58** and **61** versus **60** (EC<sub>50</sub> values of 0.094 versus 0.039 μM and 0.154 versus 0.008 μM, respectively). Once again, these analogues in Table 3 revealed that the substitution position on the morpholine moiety (such as morpholine-2-carboxylic acid vs morpholine-3-carboxylic acid), the chain length of the carboxyl group (such as formic acid vs propionic acid), and the absolute configuration of the carboxylic acid group (such as *R*-carboxylic acid vs *S*-carboxylic acid) directly influenced anti-HBV activity but had no obvious influence on hERG activity, as all of these compounds showed no sign of hERG inhibition (IC<sub>50</sub> > 30 μM). This is probably because of the introduction of the carboxyl group, which led to reduced lipophilicity and basicity or a certain amount of zwitterions.

Table 4. Relative Induction Values of the CYP3A4 Enzyme by the Selected Compounds

Comps	R	Concentration ( $\mu$ M)	% of positive control (25 $\mu$ M Rifampicin) <sup>a</sup>	Comps	R	Concentration ( $\mu$ M)	% of positive control (25 $\mu$ M Rifampicin) <sup>a</sup>
GLS4		1	41.3 (>40%)	55		1	116.9 (>40%)
( <i>R</i> )-GLS4		1	34.8 (<40%)	40		1	58.7 (>40%)
( <i>S</i> )-GLS4		1	14.8 (<40%)	57		1	79.6 (>40%)
49		1	97.4 (>40%)	62		1	23.8 (<40%)
( <i>R</i> )-49		1	103.5 (>40%)	62		10	50.8 (>40%)
( <i>S</i> )-49		1	11.8 (<40%)	46		1	35.1 (<40%)
		0.05	-1.38 (<40%)	46		10	50.5 (>40%)
53		0.2	26.8 (<40%)	58		1	24.7 (<40%)
		0.5	29 (<40%)	58		10	32.8 (<40%)
		1	84.6 (>40%)				
( <i>R</i> )-52		0.1	30.8 (<40%)				
		1	91.7 (>40%)				
		10	102.0 (>40%)				

<sup>a</sup>Experiments were done in human primary hepatocytes ( $N = 3$ ). The positive control had a minimum of a 2-fold increase in enzyme activity. The cutoff of a true inducer of P450 activity in vitro is generally considered to be 40% of the positive control.

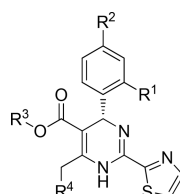
**Induction Effect of CYP3A4.** It was reported that the CYP3A4 induction of 4-*H* heteroaryldihydropyrimidine (HAP) analogues was likely related to the 4-*H* HAP core, as over 250 compounds of 4-*H* HAP were screened and most of them were found to have CYP3A4-induction liabilities.<sup>21</sup> Our previous studies also showed that most of the GLS4-like compounds possessed potent inductions of CYP3A4 enzymes (>40% increases compared with the positive control rifampicin at 10  $\mu$ M). Although the series of compounds shown in Tables 2 and 3 showed favorable potencies and decreased hERG inhibitions, we continued to investigate their CYP-enzyme-induction properties. After excluding the nonactive compounds in Tables 2 and 3 and taking into consideration the effects of different substituents on the C2, C4, and C6 positions and the effects of the chiral isomers, some representative compounds were selected for further studies of their induction activities on the CYP3A4 enzyme. As shown in Table 4, the more potent enantiomer displayed higher induction activity than the less potent enantiomer. For example, (*R*)-49 showed a 103.5% increase of CYP3A4-enzyme activity, whereas (*S*)-49, which has weaker anti-HBV activity, showed no induction (<40% increase compared with rifampicin). A similar trend was observed with the anti-HBV activities and induction abilities of the GLS4 enantiomers, *R*-GLS4 and *S*-GLS4. In addition, the compounds induced the CYP3A4 enzyme in a concentration-dependent manner. For example, compound 53 displayed no induction of CYP3A4 at lower concentrations (0.05–0.5  $\mu$ M), but it showed

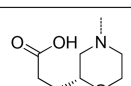
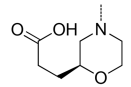
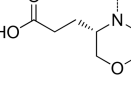
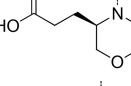
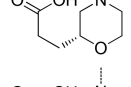
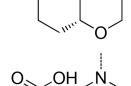
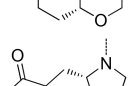
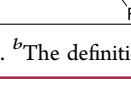
serious induction effects at the higher concentration of 1  $\mu$ M. At a concentration of 1  $\mu$ M, the selected compounds with potent anti-HBV activities, such as the morpholine-3-carboxylic acid analogue, 53; derivatives of 53 such as 55 and the carboxamide 40; and the 4,4-difluoropropanoic acid analogue, 57, also showed strong CYP3A4 inductions.

Minor variations of the C4 phenyl showed no obvious CYP3A4-induction changes, as compounds 49 (2-Cl-4-Cl), 53 (2-Br-4-F), and (*R*)-52 (2-Cl-4-F) displayed similar induction effects on CYP3A4 at the same concentration of 1  $\mu$ M. To investigate the effect of the 2-heterocycle substituent (C2 position) on CYP3A4 induction, we replaced the thiazole group with *N*-methyl imidazole to obtain compound 62. Although this compound showed no significant induction of CYP3A4 at the concentration of 1  $\mu$ M, it was found to be a strong inducer conferring a 50.8% increase at a concentration of 10  $\mu$ M. The extended carboxyl analogues of 46, which possessed a morpholine acetic acid at the C6 position, also showed dose-dependent CYP3A4 induction. In addition, it is surprising to find that compound 58, which possessed an (*R*)-morpholine-2-propionic acid at the C6 position displayed inconspicuous induction of CYP3A4 at either concentration of 1 or 10  $\mu$ M.

On the basis of the observation that the (*R*)-morpholine-2-propionic acid analogue, 58, possessed good anti-HBV activity and decreased induction of the CYP3A4 enzyme, we further tested the anti-HBV activities of several compounds with morpholine-propionic acid moieties and tested their induction

Table 5. Anti-HBV Activities and Relative Induction Values of the CYP3A4 Enzyme by Selected Compounds



Comps	R <sup>1</sup>	R <sup>2</sup>	R <sup>3</sup>	R <sup>4</sup>	EC <sub>50</sub> <sup>a</sup> ( $\mu$ M)	% of positive control <sup>b</sup> (25 $\mu$ M Rifampicin)
58	Br	F	Et		0.039	24.7 (<40%)
59	Br	F	Et		0.094	15.8 (<40%)
60	Br	F	Et		0.008	17.9 (<40%)
61	Br	F	Et		0.154	41.2 (>40%)
63	Br	F	Me		0.065	9.92 (<40%)
64	Cl	F	Me		0.087	5.99 (<40%)
65	Cl	Cl	Me		0.181	-0.01 (<40%)
66	Br	F	Et		0.085	9.19 (<40%)

<sup>a</sup>The definition of EC<sub>50</sub> is the same as that described in Table 1. <sup>b</sup>The definition of % of positive control is the same as that described in Table 4.

effects on the CYP3A4 enzyme at concentrations of 1  $\mu$ M. The results revealed that both the substitution position and stereochemistry of the propionic acid group were crucial for the anti-HBV activity and ability to induce the CYP3A4 enzyme. As shown in Table 5, the (*S*)-morpholine-2-propionic acid analogue, **59**, showed about 3-fold-reduced anti-HBV activity than **58** while displaying the same induction of the CYP3A4 enzyme as **58**. In addition, the anti-HBV activity of (*R*)-morpholine-3-propionic acid analogue **61** was 20 times lower than that of the *S*-analogue, compound **60**, but **61** showed a little more CYP3A4-enzyme induction than **60** (>40% for **61** vs 17.9% for **60**). It was also found that the methyl ester analogues, **63**, **64**, and **65**, which had different substituents on their C4 phenyls, showed decreased induction effects compared with that of **58** and lower anti-HBV activities than that of **58**. It was very fulfilling to find that the (*S*)-morpholine-3-propionic acid analogue, **60**, not only exhibited greater potency than the (*R*)-morpholine-2-propionic acid analogue, **58**, with an EC<sub>50</sub> value of 0.008  $\mu$ M, but it also displayed a weak induction effect. The (*S*)-difluoropyrrolidine-2-propionic acid analogue, **66**, had a slightly decreased induction ability and less anti-HBV activity compared with those of **60** and **58**. On the basis of the above results, we

concluded that the morpholine propionic acid played an essential role in decreasing the CYP3A4-induction capability, as unsubstituted morpholine, morpholine formic acid, and morpholine acetic acid analogues showed strong induction effects on the CYP3A4 enzyme.

**Molecular-Docking Studies.** In our previously published study, we demonstrated that GLS4 could prevent the normal assembly of core proteins and lead to aberrant formation of the capsid.<sup>24</sup> Furthermore, in an AAV-HBV model (chronic infection), GLS4 treatment significantly reduced intrahepatic Hbc levels as determined by immunohistochemistry (IHC) of liver sections (unpublished data). As derivatives of GLS4 with similar structures and in the class of 4-*H* HAP compounds, compound **58** and the other analogues were supposed to have similar mechanisms of action as GLS4.

Klumpp<sup>25</sup> has recently reported the cocrystal structure of the Cp149 Y132A-mutant hexamer in complex with compound NVR-010-001-E2 (an analogue of GLS4), which supports the result that the introduction of a morpholine group on BAY41-4109 could improve anti-HBV activity. In the article, Klumpp proposed that optimizations focusing on the replacement of this morpholine group would lead to improved protein interactions. To explore the interaction mode of the GLS4

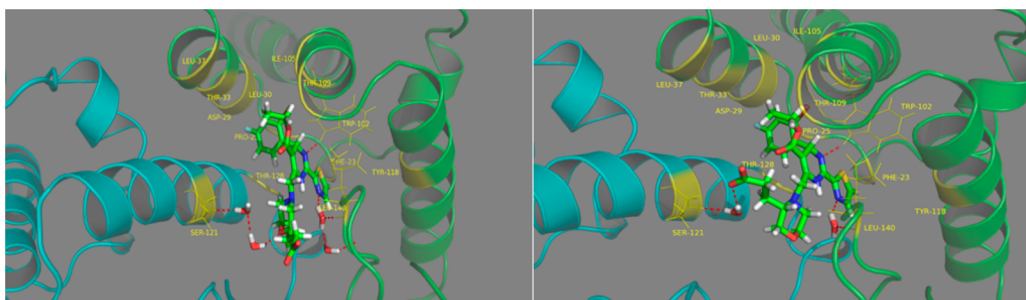


**Figure 3.** Optimal-binding model for compounds **58** (left) and **60** (right) in the active site of the capsid docked by the SURFLEX module. The ligand is shown in sticks, and some key residues are shown in lines. Hydrogen bonds are shown in dashed lines.

**Table 6.** Anti-HBV Activities, Microsome Stabilities, and Pharmacokinetics of Selected Compounds in Rats

Compd	R <sup>4</sup>	EC <sub>50</sub> <sup>a</sup> ( $\mu$ M)	HLM/MLM/DLM <sup>b</sup> (mL min <sup>-1</sup> kg <sup>-1</sup> )	dose <sup>c</sup> (mg/kg)	AUC <sub>0-24h</sub> <sup>c</sup> (h · ng/mL)	CL <sup>c</sup> (mL/min/kg)	V <sub>ss</sub> <sup>c</sup> (L/kg)	F (%) <sup>c</sup>
<b>GLS4</b>		0.014	20/485/202	iv (2) po (5)	405 90	82.2	4.85	8.9
<b>(R)-53</b>		0.010	7/377/29	iv (2) po (5)	948 548	34.9	0.4	23.1
<b>55</b>		0.005	5/89/stable	iv (2) po (5)	1610 1750	20.6	0.37	44.5
<b>58</b>		0.039	18/385/14	iv (2) po (5)	4110 4900	8.11	0.41	47.7
<b>59</b>		0.094	21/281/11	iv (2) po (5)	430 436	77.3	1.24	41
<b>60</b>		0.008	23/316/46	iv (2) po (5)	423 572	78.7	1.53	54
<b>66</b>		0.085	21/362/55	iv (2) po (5)	965 999	34.4	0.77	41.3

<sup>a</sup>The definition of EC<sub>50</sub> is the same as that described in Table 1. <sup>b</sup>Scaled intrinsic clearances in human liver microsomes (HLM), mouse liver microsomes (MLM) and dog liver microsomes (DLM). Experiments were run in duplicate, with variations of <10%. <sup>c</sup>Single-dose-pharmacokinetics (SDPK) studies of selected compounds were carried out in rats according to standard procedures. The major parameters, including the area under the curve (AUC), plasma clearance (CL), volume of distribution at steady state (V<sub>ss</sub>), and oral bioavailability (F) are reported.

analogues with the active site of the HBV capsid protein, several molecular-docking-simulation studies were carried out by using the SURFLEX module of the SYBYL package. The crystal coordinates of the capsid (PDB ID 5E0I) were downloaded from protein data bank ([www.rcsb.org](http://www.rcsb.org)), and compounds **58** and **60** were used as ligand examples.

As shown in Figure 3, both compounds are well docked in the active site of the crystal coordinate of 5E0I. For both compounds, the substituted phenyl group fits into the well-

defined, largely hydrophobic pocket created by Pro25, Asp29, Leu30, Thr33, Trp102, and Ile105, with the bromine pointing toward the protein and deep into the hydrophobic pocket. Given the limited space around the substituted phenyl group, large substituents are generally not well tolerated. The thiazole moiety on each of these two compounds is coplanar with the dihydropyrimidine core, as anticipated, and is buried in a hydrophobic environment created by the aromatic residues Phe23, Pro25, Tyr118, Trp102, and Thr128. Moreover, a

Table 7. Pharmacokinetics of GLS4 and 58 in Beagle Dogs<sup>a</sup>

compd	dose (mg/kg)	AUC <sub>0–24h</sub> (h·ng/mL)	C <sub>max</sub> (ng/mL)	C <sub>24</sub> (ng/mL)	t <sub>1/2</sub> (h)	V <sub>ss</sub> (L/kg)	CL (mL/min/kg)	F (%)
GLS4	iv (2)	1472	1423	15	17.9	15.83	16.6	23.8
	po (5)	1008	391	9	11.5			
58	iv (2)	16 540	2050	47	5.71	0.76	1.93	114.1
	po (5)	47 900	6330	232	5.1			

<sup>a</sup>Single-dose pharmacokinetics (SDPK) studies of selected compounds were carried out in beagle dogs according to standard procedures. The major parameters, including the area under the curve (AUC), maximal concentration (C<sub>max</sub>), concentration 24 h after the oral dose (C<sub>24</sub>), half-life (t<sub>1/2</sub>), plasma clearance (CL), volume of distribution at steady state (V<sub>ss</sub>), and oral bioavailability (F), are reported.

water-bridged HB network exists between the 2-thiazole and Leu140, and a  $\pi$ – $\pi$  interaction is found between the thiazole residue and Phe23. The N3 atom of the dihydropyrimidine ring forms a hydrogen bond with the main-chain nitrogen of Trp102. The ester moiety on each of these two compounds contacts the outer rim of a pocket formed by Leu37 and Thr109, so that polar and large groups may not be favored at this position. Compared with 58, 60 has achieved an approximately 5-fold improvement in antiviral activity, which can be clarified from the different binding effects of these two compounds with the core protein dimer. As shown in Figure 3, the carboxylic acid moiety of 60 makes a water-bridged HB interaction with Ser121, whereas the carboxylic acid moiety of 58 cannot make HB interactions with Ser121 in the binding site. Interestingly, the oxygen atom of the morpholino group of compound 58 could form a double water-bridged HB interaction with Ser121, though it shows reduced activity relative to that of 60. Apart from the docking simulation, which showed that compound 58 could interact with the HBV-capsid-protein dimer, the activity of compound 58 against HBV-capsid assembly was also demonstrated in an HBV-capsid-assembly-quenching assay, in which it had an IC<sub>50</sub> value of 0.14  $\mu$ M.

**Microsome Stability and PK.** On the basis of their anti-HBV activities, hERG inhibitions, and CYP3A4-enzyme inductions, a few analogues were selected for further in vitro liver-microsome-stability tests and in vivo pharmacokinetic studies in rats. Previous investigations indicated that the major metabolic pathway of GLS4 was often associated with N–C and O–C cleavages of the 6-morpholine moiety. It was hypothesized that the introduction of substituents on the morpholine would lead to decreased metabolism and improved exposure. As shown in Table 6, (R)-53 showed improved metabolic stability in three types of liver microsomes compared with that of GLS4 and correspondingly increased systemic exposure. It should be noted that the oral exposure increased much more than the exposure by the intravenous route, which suggested that the introduction of the polar carboxylic acid also led to higher aqueous solubility. Thus, compound (R)-53 displayed better oral bioavailability. In addition, compound 55, which had an additional methyl substitution on the side of the carboxylic acid, showed more metabolic stability than (R)-53 and also displayed increased systemic exposure compared with that of (R)-53 whether by intravenous (iv) or oral (po) administration. These results indicated that when the metabolic hot spots on the morpholine group of GLS4 were blocked, the plasma concentration and systemic exposure of the parent drug would increase.

In addition, both the substitution position and stereochemistry of the propionic acid group were crucial for metabolic stabilities and pharmacokinetic properties. The metabolic stabilities of the analogues with propionic acid groups (58, 59, 60, and 66) were assessed in vitro in mouse-

dog- and human-liver-microsome assays. In the experiment, all four of these compounds were more stable in the human and dog liver microsomes than in the mouse liver microsomes. Compound 60 was highly potent in vitro and showed no induction of the CYP3A4 enzyme, but its low systemic exposure prevented its further development. In addition, compounds 59 and 66 also showed higher clearances and lower systemic exposures in rats. To our delight, compound 58 displayed greatly increased systemic exposures and low clearances by both intravenous (iv) and oral (po) routes even though its metabolic stability in mouse liver microsomes was not satisfactory. We reasoned that 58 would show much higher exposure when dosed in large animals, such as beagle dogs, as it was stable in dog and human liver microsomes.

The PK profile of 58 was further evaluated in beagle dogs. As shown in Table 7, 58 exhibited longer half-lives of 5.7 h (iv) and 5.1 h (po) as well as a lower plasma clearance of 1.93 mL/min/kg, and it also showed a high systemic exposure with areas under the curves (AUC) of 16 540 h·ng/mL (iv) and 47 900 h·ng/mL (po) with an oral bioavailability (F) of 114.1%. Although the half-life of compound 58 is shorter than that of GLS4, the drug exposure and the concentration 24 h after the oral dose (C<sub>24</sub>, 232 ng/mL) for compound 58 were much higher than those of GLS4 (AUC = 1008 h·ng/mL, C<sub>24</sub> = 9 ng/mL). Considering GLS4 is dosed b.i.d. in combination with ritonavir to increase its drug exposure in the current clinical study, both once daily (q.d.) and b.i.d. dosings of compound 58 will be evaluated in the further clinical experiments to determine the best dosing regimen. The good systemic exposure and oral bioavailability of 58 in beagle dogs suggested that this compound could have desirable PK properties in human, as the liver microsome stability of 58 displayed similar tendencies in beagle dogs and human liver microsomes.

Since compound 58 demonstrated the optimal overall profile in its in vitro potency, in vitro metabolic stability, PK properties, hERG inhibition, and CYP3A4 induction, it was studied further for its induction effects on other CYP enzymes. As shown in Table 8, this compound was not a CYP1A2, CYP3A4, or CYP2B6 inducer in primary human hepatocytes as determined by the corresponding CYP1A2-, CYP3A4-, and CYP2B6-enzyme levels (<40% increases compared with the positive control) at either low concentrations of 1  $\mu$ M or higher concentrations of 10  $\mu$ M. This unique property reduces the potential risk of drug–drug interactions when HBV patients are treated.

On the basis of these results, compound 58 was selected as the candidate compound and was further assessed against HBV infections in the hydrodynamic-injection (HDI) mouse model.<sup>28</sup> In this study, female BALB/c mice were hydrodynamically injected with replication-competent HBV-DNA plasmids through the tail vein. Entecavir (ETV, 0.1 mg/kg) was used as the positive control. Twenty hours after plasmid

**Table 8. Relative Induction Values of the CYP1A2, CYP2B6, and CYP3A4 Enzymes by 58<sup>a</sup>**

enzyme subtype	concentration ( $\mu\text{M}$ )	% of positive control
1A2 positive control (omeprazole, 50 $\mu\text{M}$ )	1	4.19 (<40%)
	10	2.96 (<40%)
3A4 positive control (rifampicin, 25 $\mu\text{M}$ )	1	-13.2 (<40%)
	10	-10.6 (<40%)
2B6 positive control (phenobarbital, 1000 $\mu\text{M}$ )	1	11.8 (<40%)
	10	10.0 (<40%)

<sup>a</sup>Experiments were run in human primary hepatocytes ( $N = 3$ ). Positive controls induced a minimum of 2-fold increases in enzyme activities. The cutoff of a true positive sign of the induction of P450 activity in vitro is generally considered to be 40% of the positive control.

injection, the mice were orally dosed with a blank vehicle or different doses of compound **58** for 8 days. Plasma and liver samples were collected at the indicated time points for HBV-DNA quantification by real-time quantitative polymerase chain reaction (qPCR).

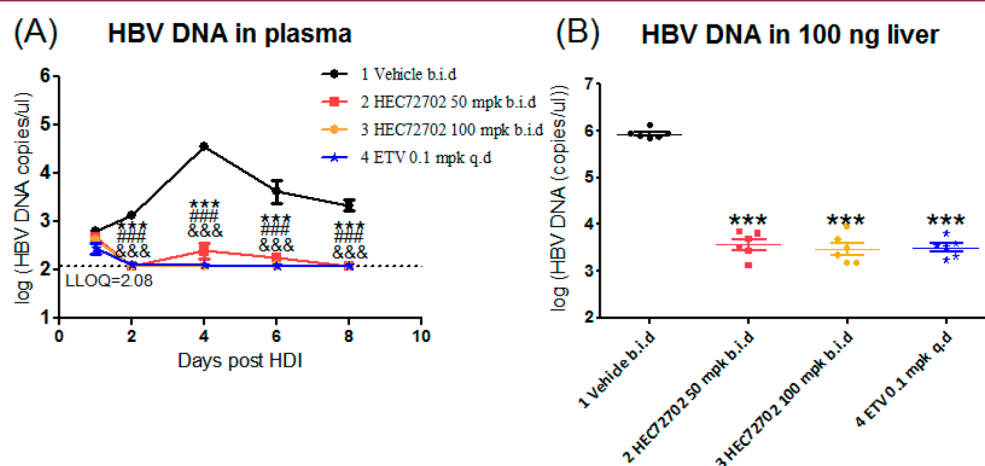
A PK study was done, and the effective dose of the compound was estimated in the same BALB/c mice prior to the anti-HBV-activity HDI experiment. Considering the short half-life of compound **58**, b.i.d. doses were chosen in the HDI mouse-model experiment. The mice were given compound **58** in a dosage of 12.5 mg/kg, and the drug concentrations in the plasma and liver were assayed at different times. The plasma  $C_{24}$  (the concentration 24 h after dosage) was 849 ng/mL and the liver  $C_{24}$  was 361 ng/g, which were much higher than the  $EC_{50}$  (0.039  $\mu\text{M}$ ) of compound **58**. Considering the plasma protein binding and linear correlation between the concentration and dosage, the dosages for the HDI mouse-model experiment were set to 50 and 100 mg/kg.

The hydrodynamic-injection mouse model was established for HBV to transiently replicate in the mouse liver. Inhibition of HBV replication can thus be studied during this transient time of about 8 days. As shown in Figure 4, **58** demonstrated a dose-

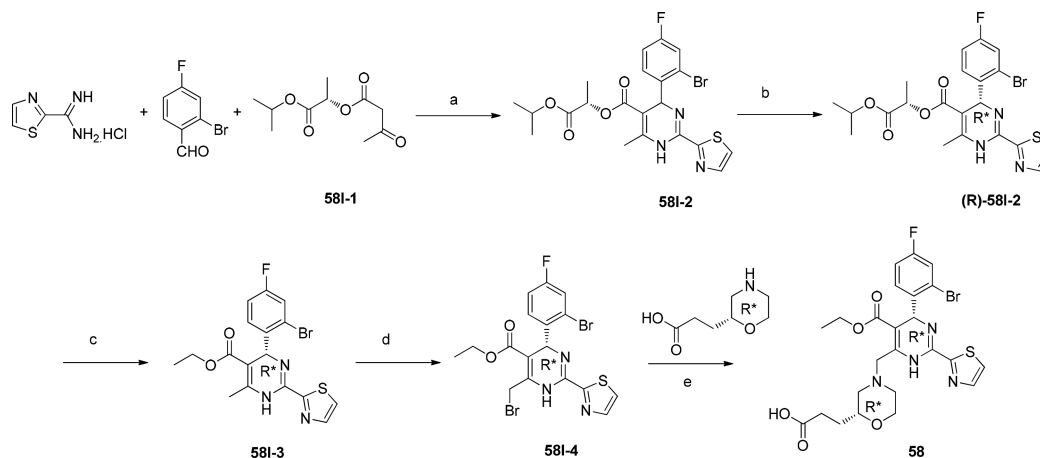
dependent reduction of HBV DNA in the plasma of infected mice when the compound was orally administered b.i.d. at 50 mg/kg (mpk), and 100 mpk, respectively. In comparison to the vehicle control group, the treatment with 50 and 100 mpk of **58** b.i.d. had achieved an over 2 log viral-load reduction in the plasma of the HDI mice on day 4. The levels of HBV DNA in the mouse livers were determined 8 days after the hydrodynamic injections of the HBV DNA plasmids. Consistent with the results in the mouse plasma, with oral dosings of compound **58** at 50 or 100 mpk b.i.d., HBV-DNA copy numbers were markedly reduced by over 100-fold in the liver, demonstrating a strong anti-HBV effect. The maximum efficacy of **58** was comparable to the maximum efficacy of ETV in this model.

It was believed that compound **58** and the other analogues of GLS4 would have activities against other HBV genotypes because of the mechanisms of action of these compounds and the conservation of the capsid protein sequence. The inhibition experiments of compound **58** against other HBV genotypes is still ongoing. Another compound, (*R*)-**52**, showed almost the same activity against four genotypes (A, B, C, and D; shown in the Supporting Information). In addition, other reported capsid inhibitors, such as JNJ-379, were also shown to be active against full-length genotype-A–H clinical isolates in vitro.<sup>31</sup>

Compound **58** exhibited low CYP inhibition, with  $IC_{50} > 10 \mu\text{M}$ , against the six major CYP enzymes (1A2, 2C9, 2D6, 3A4, 2C19, and 2B6) and was also not a time-dependent CYP inhibitor. The in vitro toxicology profiles of compound **58** were favorable, with no signs of hERG inhibition ( $IC_{50} > 30 \mu\text{M}$ ), and it was less cytotoxic to HepG2 cells, with a  $CC_{50}$  value of 96.76  $\mu\text{M}$  determined by a CellTiter-Blue assay. It was also negative in preliminary in vitro safety evaluations such as Ames as well as micronucleus-test (MNT) assays. A 14-day in vivo toxicology assessment in mice supported the further development of compound **58**, which showed a supportive safety margin as defined by the ratio of the plasma exposure ( $C_{\text{max}}$  and AUC) in mice at the NOAEL versus the exposure at the projected human efficacious dose.



**Figure 4.** Effects of treatment with **58** (HEC72702) on the inhibition of HBV replication in the HDI mouse model. Mice ( $N = 6$ ) were orally dosed with the vehicle control, compound **58** (HEC72702, 50 or 100 mpk, b.i.d.), or ETV. (A) Levels of HBV DNA in plasma. At 2, 4, 6, and 8 days postinfection, the serum HBV of all the treatment group (groups 2–4) were quantified and showed significant reductions in HBV DNA compared with that of the vehicle control. Error bar indicate the standard error of the mean ( $N = 6$ ). \*\*\* indicates  $p < 0.001$  for 50 mpk HEC72702 b.i.d. vs the vehicle, #### indicates  $p < 0.001$  for 100 mpk HEC72702 b.i.d. vs the vehicle, and &&& indicates  $p < 0.001$  for 0.1 mpk ETV q.d. vs the vehicle. (B) Quantified levels of HBV DNA in mouse livers. All the treatment groups (group 2–4) had significant reductions in liver HBV DNA compared with the vehicle control. \*\*\* indicates  $p < 0.0001$ .

Scheme 1. Synthesis of Compound 58<sup>a</sup>

<sup>a</sup>Reagents and conditions: (a) 1.2 equiv NaOAc, EtOH, reflux, 16 h; (b) recrystallization with ethanol; (c) 2 equiv Li, EtOH, reflux, 2 h; (d) 1.1 equiv NBS, CCl<sub>4</sub>, reflux, 1 h; (e) K<sub>2</sub>CO<sub>3</sub>, EtOH, 25 °C, 2 h.

The capsid inhibitor is different from nucleoside or nucleotide analogues such as tenofovir (TDF) and entecavir (ETV) in its viral inhibition mechanism. It is believed that a combination of these two kinds of drugs would benefit HBV treatment. As shown above, compound **58** displayed low CYP inhibition (IC<sub>50</sub> > 10 μM) against the six major enzymes, and it was not a CYP (1A2, 2B6 and 3A4) inducer. These properties would reduce the potential risk of drug–drug interactions of **58** and the nucleoside and nucleotide analogues. However, whether there will be drug–drug interactions needs to be further studied.

**Chemistry.** As exemplified by the synthesis of compound **58**, the synthetic approach to obtain targeted dihydropyrimidines was outlined in Scheme 1. First, a three-component reaction of thiazole-2-carboxamide hydrochloride, 2-bromo-4-fluorobenzaldehyde, and (*S*)-1-isopropoxy-1-oxopropan-2-yl 3-oxobutanoate (**58I-1**) was conducted to give the racemic dihydropyrimidine **58I-2**. After the recrystallization of the crude product of racemic dihydropyrimidine **58I-2**, the enantiomerically pure (*R*)-**58I-2** could be obtained, and the absolute stereochemistry of (*R*)-**58I-2** was unambiguously determined by an X-ray-diffraction study. The enantiomerically pure (*R*)-**58I-2** was then reacted with lithium to afford enantiomerically pure (*R*)-**58I-3** as the desired intermediate. Bromination of (*R*)-**58I-3** gave (*R*)-**58I-4**, which was finally reacted with (*R*)-3-(morpholin-2-yl) propanoic acid to provide **58** after purification. This short and concise synthetic route was successfully applied to the synthesis of the other dihydropyrimidine analogues described in this paper, which greatly facilitated and expedited our SAR studies.

## CONCLUSION

In summary, GLS4 in combination with RTV is currently in clinical phase II for chronic HBV infections and has demonstrated good efficacy. On the basis of the preclinical and clinical properties of GLS4, we obtained novel GLS4 derivatives with the appropriate anti-HBV potencies, significantly reduced hERG activities, decreased CYP enzyme inductions, and improved pharmacokinetic (PK) properties. After the extensive modification of GLS4, we have found that the morpholine carboxyl analogues showed decreased hERG activities and comparable anti-HBV activities to GLS4. With

regard to CYP-enzyme induction, we found that unsubstituted morpholine, morpholine carboxylic acid, and morpholine acetic acid analogues displayed strong CYP3A4 inductions in concentration-dependent manners, and we found that the morpholine propionic acid analogues showed decreased induction liabilities. Furthermore, the substitution position and stereochemistry of the propionic acid groups were crucial for the pharmacokinetic properties. In particular, **58**, which possessed an (*R*)-morpholine-2-propionic acid at the C6 position of the dihydropyrimidine core ring, displayed a very weak induction of CYP3A4, even at the higher concentration of 10 μM, and it also displayed a greatly increased systemic exposure and a low clearance both in rats and in beagle dogs.

Finally, compound **58** exhibited a desirable overall profile as a drug candidate in terms of its *in vitro* potency, *in vitro* metabolic stability, PK properties, and hERG inhibition. Further, it was not a CYP1A2, CYP3A4, or CYP2B6 inducer in primary human hepatocytes, avoiding the potential risk of drug–drug interactions in HBV patients. In the *in vivo* studies, compound **58** dose-dependently reduced HBV DNA in both the plasma and livers of HBV-infected HDI mice, achieving an over 2 log viral-load reduction on day 4 with 50 mpk b.i.d. dosings. Safety evaluations, including an Ames toxicity study and oral toxicity study in mice, indicated that compound **58** was safe enough. On the basis of these results, compound **58** will be selected for further development as an oral anti-HBV-infection agent.

## EXPERIMENTAL SECTION

**Synthetic-Chemistry General Comments.** All commercially available starting materials and solvents were reagent grade and used without further purification unless otherwise noted. Anhydrous THF and CH<sub>3</sub>CN were obtained by distillation over a sodium wire and CaH<sub>2</sub>, respectively. <sup>1</sup>H NMR and <sup>13</sup>C NMR spectra were recorded on a Bruker-600, Bruker-500, or Bruker-400 spectrometer (Bruker, Billerica, MA) and were referenced to the residual protio signals in CDCl<sub>3</sub> at 7.26 ppm or DMSO-*d*<sub>6</sub> at 2.50 ppm (<sup>1</sup>H NMR) and CDCl<sub>3</sub> at 77.23 ppm or DMSO-*d*<sub>6</sub> at 39.52 ppm (<sup>13</sup>C NMR). Data for NMR spectra are reported as follows: chemical shift (δ ppm), multiplicity integration (s = singlet, brs = broad singlet, d = doublet, t = triplet, q = quartet, dd = doublet of doublets, m = multiplet), coupling constant (Hz). HRMS analyses were performed on an Agilent 6530 Q-TOF mass spectrometer, and ESIMS was carried out on an Agilent 6120 mass spectrometer (Agilent Technologies, Santa Clara, CA). TLC was

performed on Huanghai HSGF 254 silica gel plates (China). Silica gel 60 H (200–300 mesh), manufactured by Qingdao Haiyang Chemical Group Company (Qingdao, China), was used for general chromatography. The purities of all the final derivatives for biological testing were confirmed to be >95%, as determined using an Agilent 1200 series HPLC instrument at 278 nm, using the following conditions: an Alltima C18 column (4.6 × 250 mm, 5 μm; Hichrom, Reading, U.K.); solvent A, 10 mM KH<sub>2</sub>PO<sub>4</sub> (pH 3.0); solvent B, acetonitrile; a gradient from 20–80% B (0 min, 20% B; 15 min, 80% B; 25 min, 80% B). Note that almost all the compounds possess similar dihydropyrimidine core structures, and representative compounds were selected for testing the <sup>13</sup>C NMR.

The synthesis and characterization of compounds 12–25 were reported in published article<sup>29</sup> and in the Supporting Information, although their hERG activities were reported in this article. For compounds 26–66, except for those described specifically, all the analogues were prepared in analogy to 58 from commercially available building blocks.

**Ethyl 4-(2-Bromo-4-fluorophenyl)-6-((1-oxidothiomorpholino)methyl)-2-(thiazol-2-yl)-1,4-dihydropyrimidine-5-carboxylate (26).** HRMS: calcd (MH<sup>+</sup>) 540.0301, exptl (MH<sup>+</sup>) 541.360. <sup>1</sup>H NMR (400 MHz, CDCl<sub>3</sub>) δ 9.51 (s, 1H), 7.85 (s, 1H), 7.47 (s, 1H), 7.34 (d, J = 6.7 Hz, 2H), 6.97 (s, 1H), 6.21 (s, 1H), 4.22 (d, J = 17.0 Hz, 1H), 4.06 (s, 2H), 3.91 (d, J = 16.7 Hz, 1H), 3.45–3.26 (m, 2H), 3.04 (s, 4H), 2.86–2.71 (m, 2H), 1.15 (t, J = 13.2 Hz, 3H). <sup>13</sup>C NMR (150 MHz, CDCl<sub>3</sub>) δ 166.02, 162.87, 162.23, 160.57, 145.13, 144.26, 143.14, 139.65, 130.51, 130.46, 129.92, 123.36, 123.69, 120.30, 120.27, 120.11, 114.98, 114.84, 98.70, 60.78, 60.05, 58.83, 56.34, 46.77, 14.14.

**Ethyl 4-(2-Bromo-4-fluorophenyl)-6-((1,1-dioxidothiomorpholino)methyl)-2-(thiazol-2-yl)-1,4-dihydropyrimidine-5-carboxylate (27).** HRMS: calcd (MH<sup>+</sup>) 556.0250, exptl (MH<sup>+</sup>) 557.0345. <sup>1</sup>H NMR (400 MHz, CDCl<sub>3</sub>) δ 9.38 (s, 1H), 7.88 (d, J = 3.0 Hz, 1H), 7.48 (d, J = 3.0 Hz, 1H), 7.35 (dd, J = 8.2, 2.1 Hz, 1H), 7.28 (t, J = 7.3 Hz, 1H), 6.97 (td, J = 8.3, 2.2 Hz, 1H), 6.22 (s, 1H), 4.34 (d, J = 17.1 Hz, 1H), 4.11–4.01 (m, 2H), 3.97 (d, J = 17.1 Hz, 1H), 3.33–3.09 (m, 8H), 1.15 (t, J = 7.1 Hz, 3H). <sup>13</sup>C NMR (150 MHz, CDCl<sub>3</sub>) δ 165.95, 162.67, 162.27, 160.61, 144.43, 144.13, 143.26, 139.48, 139.46, 130.47, 130.42, 123.42, 123.39, 123.33, 115.01, 114.87, 99.22, 60.16, 58.80, 55.13, 51.57, 51.40, 14.12.

**2-((6-(2-Bromo-4-fluorophenyl)-5-(ethoxycarbonyl)-2-(thiazol-2-yl)-3,6-dihydropyrimidin-4-yl)amino)-3-phenylpropanoic Acid (28).** HRMS: calcd (MH<sup>+</sup>) 586.0686, exptl (MH<sup>+</sup>) 587.077. <sup>1</sup>H NMR (400 MHz, DMSO-*d*<sub>6</sub>) δ 8.03 (s, 2H), 7.58 (d, J = 7.6 Hz, 1H), 7.50–7.40 (m, 1H), 7.36–7.17 (m, 6H), 5.97 (d, J = 3.5 Hz, 1H), 4.27 (s, 2H), 3.95 (q, J = 6.9 Hz, 2H), 3.30–2.99 (m, 3H), 0.05 (t, J = 7.0 Hz, 3H). <sup>13</sup>C NMR (150 MHz, DMSO-*d*<sub>6</sub>) δ 165.33, 162.34, 162.07, 160.69, 144.54, 140.52, 131.97, 129.80, 129.77, 128.95, 127.36, 122.64, 120.16, 119.99, 116.11, 115.98, 60.22, 56.50, 19.02, 14.42.

**1-((6-(2-Bromo-4-fluorophenyl)-5-(ethoxycarbonyl)-2-(thiazol-2-yl)-3,6-dihydropyrimidin-4-yl)methyl)pyrrolidine-2-carboxylic Acid (29).** HRMS: calcd (M) 536.0529, exptl (MH<sup>+</sup>) 537.0569. <sup>1</sup>H NMR (400 MHz, methanol-*d*<sub>4</sub>) δ 7.97–7.88 (m, 2H), 7.56–7.52 (m, 1H), 7.47–7.44 (m, 1H), 7.27–7.14 (m, 1H), 6.19 (s, 1H), 4.78 (d, J = 14.6 Hz, 1H), 4.54–4.38 (m, 1H), 4.30–4.17 (m, 1H), 4.11 (q, J = 7.0 Hz, 2H), 4.05–3.87 (m, 1H), 3.31–3.23 (m, 1H), 2.61–2.45 (m, 1H), 2.40–2.26 (m, 1H), 2.26–2.13 (m, 1H), 2.12–1.98 (m, 1H), 1.15 (t, J = 7.1 Hz, 3H). <sup>13</sup>C NMR (100 MHz, methanol-*d*<sub>4</sub>) δ 165.20, 163.33, 161.42, 161.38, 160.84, 144.22, 144.15, 139.04, 131.77, 131.62, 131.54, 125.30, 121.99, 121.89, 119.84, 119.80, 119.59, 119.55, 115.54, 115.48, 115.33, 115.27, 72.03, 69.22, 60.51, 55.59, 55.37, 29.01, 23.56, 13.02.

**1-((6-(2-Bromo-4-fluorophenyl)-5-(ethoxycarbonyl)-2-(thiazol-2-yl)-3,6-dihydropyrimidin-4-yl)methyl)piperidine-2-carboxylic Acid (30).** HRMS: calcd (M) 550.0686, exptl (MH<sup>+</sup>) 551.0757. <sup>1</sup>H NMR (400 MHz, methanol-*d*<sub>4</sub>) δ 7.98 (d, J = 2.9 Hz, 1H), 7.88 (s, 1H), 7.62–7.50 (m, 1H), 7.50–7.39 (m, 1H), 7.20–7.16 (m, 1H), 6.19 (s, 1H), 4.75–4.58 (m, 2H), 4.09 (q, J = 6.9 Hz, 2H), 3.96–3.51 (m, 2H), 3.24–3.11 (m, 1H), 2.30–2.10 (m, 2H), 2.03–1.72 (m, 4H), 1.14 (t, J = 7.0 Hz, 3H). <sup>13</sup>C NMR (100 MHz, methanol-*d*<sub>4</sub>) δ 166.51, 164.73, 162.73, 162.23, 145.69, 140.43, 133.12,

133.04, 126.58, 123.60, 123.50, 123.40, 121.63, 121.31, 121.20, 121.06, 120.95, 116.89, 116.78, 116.68, 116.55, 67.64, 66.75, 61.71, 58.36, 52.99, 33.09, 30.76, 23.75, 14.49.

**1-((6-(2-Bromo-4-fluorophenyl)-5-(ethoxycarbonyl)-2-(thiazol-2-yl)-3,6-dihydropyrimidin-4-yl)methyl)-4-methylpiperazine-2-carboxylic Acid (31).** HRMS: calcd (M) 565.0795, exptl (MH<sup>+</sup>) 566.0866. <sup>1</sup>H NMR (400 MHz, methanol-*d*<sub>4</sub>) δ 7.95 (s, 1H), 7.72 (s, 1H), 7.51–7.38 (m, 2H), 7.11 (t, J = 8.2 Hz, 1H), 6.14 (d, J = 10.2 Hz, 1H), 4.28–4.13 (m, 1H), 4.09–3.88 (m, 3H), 3.72–3.54 (m, 1H), 3.20–3.05 (m, 2H), 2.97–2.78 (m, 2H), 2.70–2.52 (m, 3H), 2.45 (d, J = 10.6 Hz, 2H), 1.18–1.11 (m, 3H). <sup>13</sup>C NMR (100 MHz, methanol-*d*<sub>4</sub>) δ 166.12, 162.73, 162.18, 160.25, 143.33, 143.20, 140.52, 140.04, 131.00, 123.31, 122.63, 119.41, 119.16, 114.93, 114.72, 62.17, 59.72, 59.62, 58.09, 55.16, 53.73, 53.53, 44.35, 13.18, 13.02.

**4-((6-(2-Bromo-4-fluorophenyl)-5-(ethoxycarbonyl)-2-(thiazol-2-yl)-3,6-dihydropyrimidin-4-yl)methyl)morpholine-3-carboxylic Acid (32).** HRMS: calcd (M) 552.0478, exptl (MH<sup>+</sup>) 553.0567. <sup>1</sup>H NMR (600 MHz, methanol-*d*<sub>4</sub>) δ 7.97 (t, J = 3.0 Hz, 1H), 7.79 (d, J = 2.9 Hz, 1H), 7.52–7.45 (m, 1H), 7.42 (dd, J = 8.4, 2.5 Hz, 1H), 7.12 (td, J = 8.4, 2.6 Hz, 1H), 6.17 (s, 1H), 4.55–4.43 (m, 1H), 4.35–4.25 (m, 1H), 4.17–4.00 (m, 4H), 3.96–3.81 (m, 2H), 3.75–3.64 (m, 1H), 3.47–3.35 (m, 1H), 2.83 (s, 1H), 1.15 (td, J = 7.1, 2.7 Hz, 3H). <sup>13</sup>C NMR (100 MHz, methanol-*d*<sub>4</sub>) δ 165.76, 162.93, 161.75, 160.45, 147.24, 143.57, 139.65, 131.13, 131.5, 124.10, 122.56, 122.46, 119.62, 119.38, 115.02, 114.81, 68.03, 65.73, 63.33, 62.97, 59.89, 55.05, 49.94, 13.11.

**4-((6-(2-Bromo-4-fluorophenyl)-5-(ethoxycarbonyl)-2-(thiazol-2-yl)-3,6-dihydropyrimidin-4-yl)methyl)morpholine-3-carboxylic Acid (33).** HRMS: calcd (M) 508.0983, exptl (MH<sup>+</sup>) 509.1078. <sup>1</sup>H NMR (600 MHz, methanol-*d*<sub>4</sub>) δ 7.97 (t, J = 2.9 Hz, 1H), 7.80 (d, J = 2.9 Hz, 1H), 7.53–7.45 (m, 1H), 7.24 (dd, J = 8.7, 2.4 Hz, 1H), 7.08 (td, J = 8.4, 2.6 Hz, 1H), 6.19 (s, 1H), 4.55–4.40 (m, 1H), 4.35–4.25 (m, 1H), 4.13–4.05 (m, 4H), 3.94–3.83 (m, 2H), 3.75–3.65 (m, 1H), 3.48–3.37 (m, 1H), 2.84 (s, 1H), 1.15 (td, J = 7.1, 3.1 Hz, 4H). <sup>13</sup>C NMR (100 MHz, methanol-*d*<sub>4</sub>) δ 171.32, 165.73, 163.09, 161.68, 160.61, 147.22, 143.61, 137.91, 133.21, 133.10, 131.25, 131.16, 124.13, 116.42, 116.17, 114.44, 114.23, 67.95, 65.64, 63.29, 59.92, 55.04, 49.89, 13.03.

**4-((6-(2,4-Dichlorophenyl)-5-(ethoxycarbonyl)-2-(thiazol-2-yl)-3,6-dihydropyrimidin-4-yl)methyl)morpholine-3-carboxylic Acid (34).** HRMS: calcd (M) 524.0688, exptl (MH<sup>+</sup>) 525.0771. <sup>1</sup>H NMR (600 MHz, methanol-*d*<sub>4</sub>) δ 7.97–7.96 (m, 1H), 7.79 (s, 1H), 7.51–7.41 (m, 2H), 7.32 (d, J = 8.3 Hz, 1H), 6.18 (s, 1H), 4.53–4.42 (m, 1H), 4.33–4.22 (m, 1H), 4.18–3.99 (m, 4H), 3.94–3.83 (m, 2H), 3.69 (d, J = 19.7 Hz, 1H), 3.42 (s, 1H), 2.78 (d, J = 31.5 Hz, 1H), 1.15 (td, J = 7.0, 2.8 Hz, 3H). <sup>13</sup>C NMR (150 MHz, methanol-*d*<sub>4</sub>) δ 171.59, 167.93, 165.69, 165.66, 161.65, 161.63, 147.43, 143.63, 143.58, 140.44, 133.74, 133.25, 133.15, 132.20, 130.99, 130.97, 128.97, 128.91, 128.47, 127.58, 127.51, 124.19, 67.71, 63.26, 62.91, 59.95, 55.04, 54.88, 49.89, 49.19, 13.05.

**(2R,3S)-4-((6-(2-Bromo-4-fluorophenyl)-5-(ethoxycarbonyl)-2-(thiazol-2-yl)-3,6-dihydropyrimidin-4-yl)methyl)-2-methylmorpholine-3-carboxylic Acid (35).** The synthetic procedure was described in the Supporting Information. HRMS: calcd (M) 566.0635, exptl (MH<sup>+</sup>) 567.0731. <sup>1</sup>H NMR (600 MHz, methanol-*d*<sub>4</sub>) δ 7.95 (t, J = 3.4 Hz, 1H), 7.81–7.73 (m, 1H), 7.47–7.42 (m, 1H), 7.41–7.38 (m, 1H), 7.12–7.08 (m, 1H), 6.14 (d, J = 18.0 Hz, 1H), 4.43–4.32 (m, 1H), 4.06–3.97 (m, 3H), 3.94 (d, J = 11.3 Hz, 1H), 3.89–3.78 (m, 2H), 3.21 (s, 1H), 3.01–2.78 (m, 2H), 1.32 (d, J = 6.2 Hz, 3H), 1.12 (t, J = 7.1 Hz, 3H). <sup>13</sup>C NMR (100 MHz, methanol-*d*<sub>4</sub>) δ 173.39, 167.01, 164.31, 163.12, 163.03, 161.82, 161.79, 148.37, 148.09, 145.03, 144.98, 141.18, 141.01, 140.97, 132.56, 132.48, 132.42, 125.46, 125.36, 123.97, 123.89, 123.80, 121.06, 120.98, 120.82, 120.74, 116.48, 116.39, 116.27, 116.18, 75.46, 75.31, 73.57, 73.49, 66.69, 66.52, 61.30, 57.86, 56.95, 56.63, 52.67, 52.51, 18.77, 14.50.

**4-((6-(2-Bromo-4-fluorophenyl)-5-(ethoxycarbonyl)-2-(thiazol-2-yl)-3,6-dihydropyrimidin-4-yl)methyl)-6,6-dimethylmorpholine-3-carboxylic Acid (36).** HRMS: calcd (M) 580.0791, exptl (MH<sup>+</sup>) 581.0875. <sup>1</sup>H NMR (600 MHz, methanol-*d*<sub>4</sub>) δ 7.96–7.89 (m, 1H), 7.75 (d, J = 2.8 Hz, 1H), 7.49–7.38 (m, 2H), 7.15–7.08 (m, 1H), 6.15 (d, J = 13.5 Hz, 1H), 4.18 (s, 1H), 4.13–3.97 (m, 5H), 3.43

(d,  $J = 41.7$  Hz, 1H), 3.04–2.93 (m, 1H), 2.48–72.42 (m, 1H), 1.42–1.31 (m, 6H), 1.14 (t,  $J = 7.1$  Hz, 3H).  $^{13}\text{C}$  NMR (150 MHz, MeOD)  $\delta$  176.00 (s), 167.37, 163.78, 163.30, 163.21, 162.13, 149.00, 148.72, 144.65, 144.61, 141.58, 141.39, 132.37, 132.31, 129.86, 125.15, 125.12, 124.07, 124.01, 120.97, 120.94, 120.81, 120.77, 116.25, 116.11, 72.98, 71.30, 69.10, 65.48, 64.44, 61.14, 61.12, 60.90, 59.09, 56.40, 56.07, 26.28, 26.07, 24.39, 24.13, 14.53.

**Methyl 4-((6-(2-Bromo-4-fluorophenyl)-5-(ethoxycarbonyl)-2-(thiazol-2-yl)-3,6-dihydropyrimidin-4-yl)methyl)morpholine-3-carboxylate (37).** HRMS: calcd (M) 566.0635, exptl (MH<sup>+</sup>) 567.0729.  $^1\text{H}$  NMR (400 MHz, CDCl<sub>3</sub>)  $\delta$  9.72 (d,  $J = 28.9$  Hz, 1H), 7.87 (d,  $J = 1.9$  Hz, 1H), 7.45 (d,  $J = 2.6$  Hz, 1H), 7.39–7.29 (m, 2H), 6.99–6.94 (m, 1H), 6.20 (s, 1H), 4.28 (dd,  $J = 17.6, 8.5$  Hz, 1H), 4.15–3.96 (m, 5H), 3.85 (s, 2H), 3.80 (d,  $J = 6.2$  Hz, 3H), 3.57–3.46 (m, 1H), 3.25–3.11 (m, 1H), 2.60–2.50 (m, 1H), 1.15 (t,  $J = 6.8$  Hz, 3H).  $^{13}\text{C}$  NMR (150 MHz, CDCl<sub>3</sub>)  $\delta$  171.10, 170.99, 166.17, 166.13, 163.00, 162.97, 162.18, 160.53, 146.24, 146.08, 144.50, 144.47, 143.26, 143.23, 140.00, 139.98, 139.94, 139.92, 130.70, 130.64, 130.57, 130.51, 123.31, 123.25, 123.21, 123.15, 123.00, 122.97, 120.20, 120.10, 120.03, 119.94, 114.99, 114.91, 114.85, 114.77, 98.12, 97.93, 69.18, 67.29, 62.76, 62.66, 59.91, 59.89, 58.91, 58.75, 55.03, 54.84, 52.13, 49.82, 49.17, 14.16.

**Isopropyl 4-((6-(2-Bromo-4-fluorophenyl)-5-(ethoxycarbonyl)-2-(thiazol-2-yl)-3,6-dihydropyrimidin-4-yl)methyl)morpholine-3-carboxylate (38).** HRMS: calcd (M) 594.0948, exptl (MH<sup>+</sup>) 595.1021.  $^1\text{H}$  NMR (400 MHz, methanol-*d*<sub>4</sub>)  $\delta$  7.97 (d,  $J = 2.1$  Hz, 1H), 7.75 (d,  $J = 2.0$  Hz, 1H), 7.41 (d,  $J = 8.1$  Hz, 2H), 7.11–7.07 (m, 1H), 6.16 (s, 1H), 5.15–5.06 (m, 1H), 4.32 ( $J = 14.9$  Hz, 1H), 4.12–3.98 (m, 5H), 3.83 (s, 2H), 3.55 (d,  $J = 35.9$  Hz, 1H), 3.24–3.11 (m, 1H), 2.61–2.50 (m, 1H), 1.27 (d,  $J = 6.1$  Hz, 6H), 1.15 (t,  $J = 7.0$  Hz, 3H).  $^{13}\text{C}$  NMR (150 MHz, methanol-*d*<sub>4</sub>)  $\delta$  171.78, 171.71, 167.43, 163.73, 163.47, 163.42, 162.08, 148.29, 148.15, 146.49, 146.39, 144.62, 144.59, 141.42, 141.40, 132.19, 132.13, 125.03, 124.23, 124.16, 120.94, 120.78, 116.18, 116.04, 99.05, 98.96, 70.35, 70.29, 70.14, 70.04, 68.41, 64.16, 63.95, 61.06, 59.92, 59.87, 56.10, 55.84, 50.76, 50.20, 49.14, 49.00, 48.86, 22.10, 22.09, 22.07, 22.05, 14.57.

**Ethyl 4-(2-Bromo-4-fluorophenyl)-6-((3-carbamoylmorpholino)methyl)-2-(thiazol-2-yl)-1,4-dihydropyrimidine-5-carboxylate (39).** HRMS: calcd (M) 551.0638, exptl (MH<sup>+</sup>) 552.0726.  $^1\text{H}$  NMR (400 MHz, methanol-*d*<sub>4</sub>)  $\delta$  7.99–7.94 (m, 1H), 7.74 (s, 1H), 7.50–7.35 (m, 2H), 7.16–7.05 (m, 1H), 6.15 (d,  $J = 10.3$  Hz, 1H), 4.21 (q, 11.6 Hz, 1H), 4.11–3.97 (m, 3H), 3.93–3.69 (m, 4H), 3.09–2.87 (m, 1H), 2.65–2.47 (m, 1H), 1.47 (s, 1H), 1.15 (t,  $J = 7.2$  Hz, 3H).  $^{13}\text{C}$  NMR (100 MHz, methanol-*d*<sub>4</sub>)  $\delta$  174.80, 167.47, 163.59, 161.74, 146.65, 144.63, 139.61, 132.30, 132.22, 131.25, 124.93, 123.51, 121.01, 120.94, 120.76, 120.70, 116.29, 116.28, 116.22, 116.17, 116.07, 116.01, 70.61, 68.03, 66.80, 61.11, 59.72, 55.13, 52.68, 52.56, 14.52.

**Ethyl 4-(2-Bromo-4-fluorophenyl)-6-((3-(methylcarbamoyl)morpholino)methyl)-2-(thiazol-2-yl)-1,4-dihydropyrimidine-5-carboxylate (40).** HRMS: calcd (M) 565.0795, exptl (MH<sup>+</sup>) 566.0886.  $^1\text{H}$  NMR (400 MHz, methanol-*d*<sub>4</sub>)  $\delta$  7.98 (d,  $J = 2.8$  Hz, 1H), 7.74 (s, 1H), 7.51–7.36 (m, 2H), 7.10 (t,  $J = 8.2$  Hz, 1H), 6.15 (d,  $J = 10.5$  Hz, 1H), 4.27–3.99 (m, 3H), 3.99–3.68 (m, 5H), 3.31–3.23 (m, 1H), 3.07–2.85 (m, 1H), 2.78 (d,  $J = 20.5$  Hz, 3H), 2.62–2.49 (m, 1H), 1.14 (td,  $J = 6.8, 2.0$  Hz, 3H).  $^{13}\text{C}$  NMR (100 MHz, methanol-*d*<sub>4</sub>)  $\delta$  171.29, 166.04, 162.15, 146.37, 146.29, 143.23, 130.94, 130.86, 123.55, 123.29, 122.68, 119.59, 119.29, 114.85, 114.64, 98.49, 69.09, 68.81, 66.58, 66.49, 65.82, 59.70, 58.32, 53.54, 51.34, 24.92, 13.12.

**Ethyl 4-(2-Bromo-4-fluorophenyl)-6-((3-((methylsulfonyl)carbamoyl)morpholino)methyl)-2-(thiazol-2-yl)-1,4-dihydropyrimidine-5-carboxylate (41).** The synthetic procedure was described in the Supporting Information. HRMS: calcd (M) 629.0414, exptl (MH<sup>+</sup>) 630.0525.  $^1\text{H}$  NMR (600 MHz, methanol-*d*<sub>4</sub>)  $\delta$  7.97 (d,  $J = 3.0$  Hz, 1H), 7.79 (d,  $J = 2.9$  Hz, 1H), 7.53–7.45 (m, 1H), 7.45–7.38 (m, 1H), 7.13 (td,  $J = 8.4, 2.3$  Hz, 1H), 6.17 (d,  $J = 3.9$  Hz, 1H), 4.40 (d,  $J = 16.9$  Hz, 1H), 4.17–4.03 (m, 4H), 3.93–3.81 (m, 3H), 3.58 (s, 1H), 3.31–3.16 (m, 4H), 2.76 (s, 1H), 1.15 (t,  $J = 7.1$  Hz, 3H).  $^{13}\text{C}$  NMR (150 MHz, MeOD)  $\delta$  172.76, 167.16, 163.90, 163.15, 162.24, 148.49, 144.93, 140.98, 132.61, 132.56, 132.38, 129.88,

125.48, 123.91, 123.84, 121.03, 120.92, 120.87, 120.76, 116.49, 116.35, 116.23, 72.90, 69.49, 67.37, 66.65, 66.13, 65.63, 61.29, 55.93, 51.85, 51.31, 14.52.

**Ethyl 4-(2,4-Dichlorophenyl)-6-((3-(hydroxymethyl)morpholino)methyl)-2-(thiazol-2-yl)-1,4-dihydropyrimidine-5-carboxylate (42).** HRMS: calcd (M) 510.0895, exptl (MH<sup>+</sup>) 511.0973.  $^1\text{H}$  NMR (400 MHz, methanol-*d*<sub>4</sub>)  $\delta$  7.96 (d,  $J = 2.1$  Hz, 1H), 7.75 (d,  $J = 2.5$  Hz, 1H), 7.51–7.36 (m, 2H), 7.30 (d,  $J = 7.8$  Hz, 1H), 6.18 (s, 1H), 4.36–4.23 (m, 1H), 4.15–4.01 (m, 3H), 3.94 (d,  $J = 8.6$  Hz, 1H), 3.85–3.62 (m, 5H), 2.95–2.75 (m, 1H), 2.74–2.51 (m, 2H), 1.15 (t,  $J = 7.0$  Hz, 3H).  $^{13}\text{C}$  NMR (100 MHz, methanol-*d*<sub>4</sub>)  $\delta$  175.16, 167.03, 164.30, 163.13, 163.10, 161.82, 147.93, 144.92, 141.05, 141.02, 132.48, 132.44, 132.39, 132.35, 125.54, 125.51, 123.99, 123.97, 123.90, 123.87, 121.07, 120.82, 116.42, 116.40, 116.21, 116.19, 111.37, 75.59, 75.33, 66.26, 66.05, 61.51, 61.34, 57.97, 56.07, 55.82, 53.92, 53.72, 14.51.

**Ethyl 4-(2-Bromo-4-fluorophenyl)-6-((2-(hydroxymethyl)morpholino)methyl)-2-(thiazol-2-yl)-1,4-dihydropyrimidine-5-carboxylate (43).** HRMS: calcd (M) 538.0686, exptl (MH<sup>+</sup>) 539.0753.  $^1\text{H}$  NMR (400 MHz, CDCl<sub>3</sub>)  $\delta$  9.62 (d,  $J = 7.1$  Hz, 1H), 7.86 (d,  $J = 2.9$  Hz, 1H), 7.46 (d,  $J = 3.0$  Hz, 1H), 7.37–7.29 (m, 2H), 6.97 (t,  $J = 8.1$  Hz, 1H), 6.21 (s, 1H), 4.16–3.97 (m, 4H), 3.94–3.80 (m, 3H), 3.77–3.57 (m, 2H), 2.85–2.75 (m, 1H), 2.68 (t,  $J = 11.2$  Hz, 1H), 2.50–2.30 (m, 1H), 2.06 (s, 1H), 1.15 (t,  $J = 7.1$  Hz, 3H).  $^{13}\text{C}$  NMR (150 MHz, CDCl<sub>3</sub>)  $\delta$  166.15, 162.92, 162.21, 160.55, 145.86, 145.82, 144.37, 144.36, 143.20, 143.19, 139.89, 139.87, 139.84, 130.56, 130.51, 123.31, 123.25, 123.11, 123.09, 120.21, 120.05, 114.98, 114.84, 109.99, 98.33, 98.28, 76.11, 66.63, 66.55, 63.78, 59.93, 58.78, 58.77, 56.63, 54.85, 54.57, 53.34, 53.06, 14.15.

**4-((6-(2-Bromo-4-fluorophenyl)-5-(ethoxycarbonyl)-2-(thiazol-2-yl)-3,6-dihydropyrimidin-4-yl)methyl)morpholine-2-carboxylic Acid (44).** HRMS: calcd (M) 552.0478, exptl (MH<sup>+</sup>) 553.0542.  $^1\text{H}$  NMR (400 MHz, methanol-*d*<sub>4</sub>)  $\delta$  7.95 (s, 1H), 7.77 (s, 1H), 7.53–7.36 (m, 2H), 7.12 (t,  $J = 6.8$  Hz, 1H), 6.17 (s, 1H), 4.41–4.21 (m, 2H), 4.18–4.06 (m, 4H), 3.89 (t,  $J = 8.8$  Hz, 1H), 3.49–3.24 (m, 1H), 3.01 (t,  $J = 14.0$  Hz, 1H), 2.92–2.69 (m, 2H), 1.14 (t,  $J = 6.3$  Hz, 3H).  $^{13}\text{C}$  NMR (100 MHz, methanol-*d*<sub>4</sub>)  $\delta$  175.16, 167.03, 164.30, 163.13, 163.10, 161.82, 147.93, 144.92, 141.05, 141.02, 132.48, 132.44, 132.39, 132.35, 125.54, 125.51, 123.99, 123.97, 123.90, 123.87, 121.07, 120.82, 116.42, 116.21, 116.19, 111.37, 75.59, 75.33, 66.26, 66.05, 61.51, 61.34, 57.97, 56.07, 55.82, 53.92, 53.72, 14.51.

**2-(4-((6-(2-Bromo-4-fluorophenyl)-5-(ethoxycarbonyl)-2-(thiazol-2-yl)-3,6-dihydropyrimidin-4-yl)methyl)morpholin-3-yl)acetic Acid (45).** HRMS: calcd (M) 566.0636, exptl (MH<sup>+</sup>) 567.0713.  $^1\text{H}$  NMR (600 MHz, methanol-*d*<sub>4</sub>)  $\delta$  7.96 (s, 1H), 7.77 (s, 1H), 7.52–7.38 (m, 2H), 7.11 (t,  $J = 7.2$  Hz, 1H), 6.17 (s, 1H), 4.40–4.04 (m, 4H), 4.02–3.71 (m, 4H), 3.23 (s, 1H), 3.04 (s, 1H), 2.70–2.65 (m, 3H), 1.22–1.08 (m, 3H).  $^{13}\text{C}$  NMR (150 MHz, methanol-*d*<sub>4</sub>)  $\delta$  174.25, 165.84, 162.46, 161.91, 160.78, 147.27, 143.40, 139.79, 131.00, 123.97, 122.61, 119.59, 119.55, 119.41, 119.38, 114.95, 114.81, 69.48, 59.83, 56.61, 53.20, 53.16, 52.84, 50.46, 49.84, 13.12.

**2-(4-((6-(2-Bromo-4-fluorophenyl)-5-(ethoxycarbonyl)-2-(thiazol-2-yl)-3,6-dihydropyrimidin-4-yl)methyl)morpholin-2-yl)acetic Acid (46).** HRMS: calcd (M) 566.0635, exptl (MH<sup>+</sup>) 567.0729.  $^1\text{H}$  NMR (600 MHz, methanol-*d*<sub>4</sub>)  $\delta$  7.96 (d,  $J = 3.1$  Hz, 1H), 7.76 (d,  $J = 2.9$  Hz, 1H), 7.46–7.40 (m, 2H), 7.16–7.10 (m, 1H), 6.17 (s, 1H), 4.14–4.04 (m, 4H), 3.98–3.91 (m, 2H), 3.86–3.81 (m, 1H), 3.09 (s, 1H), 2.77 (s, 1H), 2.61–2.43 (m, 3H), 2.32 (s, 1H), 1.15 (t,  $J = 7.1$  Hz, 3H).  $^{13}\text{C}$  NMR (100 MHz, methanol-*d*<sub>4</sub>)  $\delta$  174.62, 167.33, 164.22, 163.33, 161.74, 144.69, 141.24, 132.28, 132.19, 125.12, 124.12, 121.00, 120.75, 116.37, 116.16, 73.93, 67.52, 61.16, 59.04, 57.59, 54.01, 39.55, 14.52.

**3-(4-((6-(2-Bromo-4-fluorophenyl)-5-(ethoxycarbonyl)-2-(thiazol-2-yl)-3,6-dihydropyrimidin-4-yl)methyl)morpholin-3-yl)propanoic Acid (47).** HRMS: calcd (M) 580.0791, exptl (MH<sup>+</sup>) 581.0861.  $^1\text{H}$  NMR (600 MHz, acetone-*d*<sub>6</sub>)  $\delta$  9.94 (s, 1H), 7.98 (d,  $J = 3.1$  Hz, 1H), 7.80 (d,  $J = 3.1$  Hz, 1H), 7.54–7.52 (m, 1H), 7.42 (dd,  $J = 8.5, 2.6$  Hz, 1H), 7.15 (td,  $J = 8.5, 2.6$  Hz, 1H), 6.18 (s, 1H), 4.32 (d,  $J = 18.1$  Hz, 1H), 4.05–4.01 (m, 3H), 3.93 (dd,  $J = 11.4, 2.8$  Hz, 1H), 3.83–3.80 (m, 1H), 3.74–3.70 (m, 1H), 3.50–3.47 (m, 1H), 2.92–2.86 (m, 1H), 2.67–2.61 (m, 2H), 2.52–2.47 (m, 1H), 2.45–2.37 (m,

1H), 2.11–2.08 (m, 1H), 1.85–1.80 (m, 1H), 1.13 (t,  $J = 7.1$  Hz, 3H).  $^{13}\text{C}$  NMR (150 MHz, acetone- $d_6$ )  $\delta$  173.59, 165.45, 162.83, 162.11, 160.47, 147.63, 144.17, 143.48, 140.71, 131.29, 131.23, 123.73, 122.84, 122.78, 119.54, 119.38, 115.34, 115.20, 96.43, 70.08, 66.78, 59.80, 59.67, 59.28, 58.69, 53.49, 53.45, 52.41, 13.66.

**3-(4-((6-(2-Bromo-4-fluorophenyl)-5-(ethoxycarbonyl)-2-(thiazol-2-yl)-3,6-dihydropyrimidin-4-yl)methyl)morpholin-2-yl)propanoic Acid (48)**. HRMS: calcd (M) 580.0791, exptl (MH<sup>+</sup>) 581.086.  $^1\text{H}$  NMR (600 MHz, acetone- $d_6$ )  $\delta$  9.72 (s, 1H), 7.97 (d,  $J = 2.9$  Hz, 1H), 7.79 (t,  $J = 3.2$  Hz, 1H), 7.53–7.49 (m, 1H), 7.44 (dd,  $J = 8.5, 2.5$  Hz, 1H), 7.15–7.11 (m, 1H), 6.19 (s, 1H), 4.10–3.99 (m, 3H), 3.97–3.88 (m, 2H), 3.75–3.71 (m, 1H), 3.69–3.65 (m, 1H), 2.99–2.73 (m, 2H), 2.51–2.33 (m, 3H), 2.23 (t,  $J = 10.5$  Hz, 1H), 1.84–1.71 (m, 2H), 1.13 (t,  $J = 7.1$  Hz, 3H).  $^{13}\text{C}$  NMR (150 MHz, acetone- $d_6$ )  $\delta$  173.63, 173.55, 165.38, 162.77, 162.73, 162.15, 160.50, 146.46, 146.40, 144.24, 144.22, 143.47, 143.45, 140.60, 131.14, 131.11, 131.09, 131.05, 123.75, 123.70, 122.94, 122.90, 122.88, 119.66, 119.49, 115.14, 115.10, 115.00, 114.96, 97.76, 97.62, 74.83, 74.80, 66.47, 66.40, 59.35, 59.34, 58.76, 58.73, 58.49, 58.30, 56.35, 56.28, 53.27, 53.03, 13.64.

**(3S)-4-((6-(2,4-Dichlorophenyl)-5-(ethoxycarbonyl)-2-(thiazol-2-yl)-3,6-dihydropyrimidin-4-yl)methyl)morpholine-3-carboxylic Acid (49)**. HRMS: calcd (M) 524.0688, exptl (MH<sup>+</sup>) 525.0749.  $^1\text{H}$  NMR (600 MHz, methanol- $d_4$ )  $\delta$  8.00–7.94 (m, 1H), 7.79 (s, 1H), 7.48 (s, 1H), 7.45 (t,  $J = 9.3$  Hz, 1H), 7.31 (d,  $J = 8.4$  Hz, 1H), 6.18 (s, 1H), 4.53–4.42 (m, 1H), 4.35–4.23 (m, 1H), 4.17–4.09 (m, 1H), 4.08–4.04 (m, 3H), 3.93–3.84 (m, 2H), 3.69 (d,  $J = 19.4$  Hz, 1H), 3.42 (s, 1H), 2.79 (d,  $J = 26.1$  Hz, 1H), 1.15 (td,  $J = 7.1, 2.8$  Hz, 3H).  $^{13}\text{C}$  NMR (100 MHz, methanol- $d_4$ )  $\delta$  172.80, 167.07, 167.04, 163.04, 163.02, 148.81, 148.77, 144.99, 144.94, 141.87, 141.82, 135.09, 134.62, 134.53, 132.34, 130.34, 130.28, 128.95, 128.88, 125.55, 69.40, 69.28, 67.10, 64.67, 64.33, 61.34, 56.42, 56.27, 51.28, 50.62, 14.44.

**(S)-4-(((R)-6-(2,4-Dichlorophenyl)-5-(ethoxycarbonyl)-2-(thiazol-2-yl)-3,6-dihydropyrimidin-4-yl)methyl)morpholine-3-carboxylic Acid ((R)-49)**. HRMS: calcd (M) 524.0688, exptl (MH<sup>+</sup>) 525.0771.  $^1\text{H}$  NMR (400 MHz, methanol- $d_4$ )  $\delta$  7.94 (d,  $J = 2.1$  Hz, 1H), 7.76 (d,  $J = 1.6$  Hz, 1H), 7.44 (d,  $J = 12.0$  Hz, 2H), 7.28 (d,  $J = 8.1$  Hz, 1H), 6.18 (s, 1H), 4.52 (d,  $J = 17.1$  Hz, 1H), 4.27 (d,  $J = 17.1$  Hz, 1H), 4.15–4.02 (m, 4H), 3.87 (s, 2H), 3.70 (s, 1H), 3.42 (s, 1H), 2.76 (d,  $J = 8.1$  Hz, 1H), 1.14 (t,  $J = 6.9$  Hz, 3H).  $^{13}\text{C}$  NMR (150 MHz, methanol- $d_4$ )  $\delta$  172.93, 167.01, 163.00, 148.85, 144.95, 141.86, 135.08, 134.58, 132.36, 130.32, 128.89, 125.60, 69.20, 66.94, 64.31, 61.51, 61.34, 55.93, 50.63, 14.45.

**(S)-4-(((S)-6-(2,4-Dichlorophenyl)-5-(ethoxycarbonyl)-2-(thiazol-2-yl)-3,6-dihydropyrimidin-4-yl)methyl)morpholine-3-carboxylic Acid ((S)-49)**. HRMS: calcd (M) 524.0688, exptl (MH<sup>+</sup>) 525.0790.  $^1\text{H}$  NMR (600 MHz, methanol- $d_4$ )  $\delta$  8.22 (dd,  $J = 18.6, 3.0$  Hz, 2H), 7.55 (dd,  $J = 5.2, 3.1$  Hz, 2H), 7.42 (dd,  $J = 8.4, 2.0$  Hz, 1H), 6.32 (s, 1H), 5.08 (d,  $J = 17.2$  Hz, 1H), 4.42 (d,  $J = 11.4$  Hz, 1H), 4.08 (q,  $J = 7.1$  Hz, 2H), 3.95 (dd,  $J = 12.3, 3.5$  Hz, 1H), 3.81–3.78 (m, 2H), 3.75–3.69 (m, 1H), 3.39–3.34 (m, 1H), 3.08 (s, 1H), 2.92–2.87 (m, 1H), 1.15–1.13 (m, 3H).  $^{13}\text{C}$  NMR (100 MHz, methanol- $d_4$ )  $\delta$  175.16, 167.03, 164.30, 163.13, 163.10, 161.82, 147.93, 144.92, 141.05, 141.02, 132.48, 132.44, 132.39, 132.35, 125.54, 125.51, 123.99, 123.97, 123.90, 123.87, 121.07, 120.82, 116.42, 116.40, 116.21, 116.19, 111.37, 106.06, 75.59, 75.33, 66.26, 66.05, 61.51, 61.34, 57.97, 56.07, 55.82, 53.92, 53.72, 14.51.

**(3R)-4-((6-(2,4-Dichlorophenyl)-5-(ethoxycarbonyl)-2-(thiazol-2-yl)-3,6-dihydropyrimidin-4-yl)methyl)morpholine-3-carboxylic Acid ((R)-50)**. HRMS: calcd (M) 524.0688, exptl (MH<sup>+</sup>) 525.0761.  $^1\text{H}$  NMR (400 MHz, methanol- $d_4$ )  $\delta$  8.02 (d,  $J = 3.0$  Hz, 1H), 7.88 (d,  $J = 3.0$  Hz, 1H), 7.51 (d,  $J = 8.6$  Hz, 2H), 7.35 (d,  $J = 8.4$  Hz, 1H), 6.21 (s, 1H), 4.58–4.42 (m, 2H), 4.17 (dd,  $J = 11.9, 3.4$  Hz, 1H), 4.13–4.04 (m, 3H), 4.00–3.86 (m, 3H), 3.53–3.46 (m, 1H), 3.04–2.93 (m, 1H), 1.16 (t,  $J = 7.1$  Hz, 3H).  $^{13}\text{C}$  NMR (150 MHz, CDCl<sub>3</sub>)  $\delta$  171.30, 165.05, 159.98, 147.72, 146.78, 143.97, 138.80, 134.62, 133.24, 130.81, 129.67, 127.98, 125.28, 68.00, 65.73, 63.48, 60.76, 55.35, 53.11, 50.28, 13.95.

**(R)-4-(((S)-6-(2,4-Dichlorophenyl)-5-(ethoxycarbonyl)-2-(thiazol-2-yl)-3,6-dihydropyrimidin-4-yl)methyl)morpholine-3-carboxylic Acid ((S)-50)**. HRMS: calcd (M) 524.0688, exptl (MH<sup>+</sup>)

525.0722.  $^1\text{H}$  NMR (400 MHz, methanol- $d_4$ )  $\delta$  7.94 (s, 1H), 7.73 (s, 1H), 7.43 (d,  $J = 9.5$  Hz, 2H), 7.29 (d,  $J = 7.9$  Hz, 1H), 6.16 (s, 1H), 4.17–3.95 (m, 5H), 3.93–3.77 (m, 2H), 3.74–3.68 (m, 1H), 3.51 (s, 1H), 3.30–3.16 (m, 2H), 1.14 (t,  $J = 6.8$  Hz, 3H).  $^{13}\text{C}$  NMR (100 MHz, methanol- $d_4$ )  $\delta$  172.96, 167.11, 163.09, 148.80, 144.92, 141.89, 135.09, 134.65, 132.32, 130.35, 128.87, 125.50, 69.35, 67.11, 64.33, 61.51, 61.33, 56.28, 50.61, 14.44.

**(3S)-4-(((6-(2-Chloro-4-fluorophenyl)-5-(ethoxycarbonyl)-2-(thiazol-2-yl)-3,6-dihydropyrimidin-4-yl)methyl)morpholine-3-carboxylic Acid (51)**. HRMS: calcd (M) 508.0983, exptl (MH<sup>+</sup>) 509.1089.  $^1\text{H}$  NMR (600 MHz, methanol- $d_4$ )  $\delta$  7.97 (t,  $J = 2.8$  Hz, 1H), 7.80 (d,  $J = 2.7$  Hz, 1H), 7.51–7.45 (m, 1H), 7.24 (dt,  $J = 8.7, 2.5$  Hz, 1H), 7.10–7.05 (m, 1H), 6.19 (s, 1H), 4.54–4.44 (m, 1H), 4.32–4.25 (m, 1H), 4.17–4.02 (m, 4H), 3.95–3.83 (m, 2H), 3.69 (d,  $J = 16.4$  Hz, 1H), 3.44 (s, 1H), 2.83 (s, 1H), 1.15 (td,  $J = 7.1, 2.6$  Hz, 3H).  $^{13}\text{C}$  NMR (100 MHz, methanol- $d_4$ )  $\delta$  172.85, 167.09, 164.46, 163.04, 161.99, 148.67, 145.02, 144.97, 139.34, 134.66, 134.57, 134.47, 132.66, 132.57, 125.56, 117.87, 117.81, 117.62, 117.56, 115.86, 115.79, 115.65, 115.58, 69.33, 66.99, 64.83, 64.48, 56.45, 56.29, 51.32, 50.68, 14.44.

**(3S)-4-(((6-(2-Chloro-4-fluorophenyl)-5-(methoxycarbonyl)-2-(thiazol-2-yl)-3,6-dihydropyrimidin-4-yl)methyl)morpholine-3-carboxylic Acid (52)**. HRMS: calcd (M) 494.0827, exptl (MH<sup>+</sup>) 495.0931.  $^1\text{H}$  NMR (600 MHz, methanol- $d_4$ )  $\delta$  7.97 (t,  $J = 2.6$  Hz, 1H), 7.79 (d,  $J = 2.7$  Hz, 1H), 7.50–7.44 (m, 1H), 7.24 (dt,  $J = 8.7, 2.4$  Hz, 1H), 7.08–7.04 (m, 1H), 6.17 (s, 1H), 4.52–4.42 (m, 1H), 4.34–4.22 (m, 1H), 4.16–4.00 (m, 2H), 3.95–3.83 (m, 2H), 3.70–3.67 (m, 1H), 3.62 (s, 3H), 3.42 (s, 1H), 2.82 (s, 1H).  $^{13}\text{C}$  NMR (100 MHz, methanol- $d_4$ )  $\delta$  172.92, 167.60, 164.47, 163.07, 162.00, 148.80, 144.99, 144.95, 139.06, 134.73, 134.65, 134.55, 132.50, 132.40, 125.50, 117.97, 117.90, 117.72, 117.65, 115.81, 115.75, 115.60, 115.54, 73.53, 69.46, 67.12, 64.79, 64.47, 62.27, 56.42, 56.32, 51.72, 51.36, 14.40.

**(S)-4-(((R)-6-(2-Chloro-4-fluorophenyl)-5-(methoxycarbonyl)-2-(thiazol-2-yl)-3,6-dihydropyrimidin-4-yl)methyl)morpholine-3-carboxylic Acid ((R)-52)**. HRMS: calcd (M) 494.0827, exptl (MH<sup>+</sup>) 495.0910.  $^1\text{H}$  NMR (600 MHz, methanol- $d_4$ )  $\delta$  7.97 (d,  $J = 3.1$  Hz, 1H), 7.79 (d,  $J = 3.0$  Hz, 1H), 7.47–7.45 (m, 1H), 7.24 (dd,  $J = 8.7, 2.5$  Hz, 1H), 7.06 (td,  $J = 8.4, 2.5$  Hz, 1H), 6.17 (s, 1H), 4.52 (d,  $J = 16.8$  Hz, 1H), 4.28 (d,  $J = 16.3$  Hz, 1H), 4.16–4.06 (m, 2H), 3.93–3.85 (m, 2H), 3.71 (s, 1H), 3.62 (s, 3H), 3.44 (s, 1H), 2.78 (s, 1H).  $^{13}\text{C}$  NMR (150 MHz, methanol- $d_4$ )  $\delta$  171.58, 166.16, 162.68, 161.63, 161.03, 147.54, 143.61, 137.74, 133.29, 133.22, 131.10, 131.04, 124.22, 116.54, 116.38, 114.36, 114.22, 67.82, 65.48, 63.01, 60.14, 54.95, 50.36, 49.29.

**(3S)-4-(((6-(2-Bromo-4-fluorophenyl)-5-(ethoxycarbonyl)-2-(thiazol-2-yl)-3,6-dihydropyrimidin-4-yl)methyl)morpholine-3-carboxylic Acid (53)**. HRMS: calcd (M) 552.0478, exptl (MH<sup>+</sup>) 553.0568.  $^1\text{H}$  NMR (600 MHz, methanol- $d_4$ )  $\delta$  7.97 (t,  $J = 2.8$  Hz, 1H), 7.79 (t,  $J = 2.7$  Hz, 1H), 7.52–7.45 (m, 1H), 7.42 (dt,  $J = 8.4, 2.5$  Hz, 1H), 7.14–7.10 (m, 1H), 6.17 (s, 1H), 4.55–4.44 (m, 1H), 4.38–4.23 (m, 1H), 4.17–4.01 (m, 4H), 3.95–3.84 (m, 2H), 3.70 (d,  $J = 17.6$  Hz, 1H), 3.53–3.36 (m, 1H), 2.84–2.73 (m, 1H), 1.15 (td,  $J = 7.1, 2.4$  Hz, 3H).  $^{13}\text{C}$  NMR (100 MHz, methanol- $d_4$ )  $\delta$  174.31, 167.27, 164.23, 163.29, 163.24, 161.75, 148.83, 147.90, 144.90, 144.88, 141.30, 141.17, 141.14, 132.52, 132.44, 132.35, 125.22, 123.94, 123.85, 121.00, 120.91, 120.75, 120.66, 116.39, 116.33, 116.18, 116.12, 100.84, 70.00, 69.72, 67.40, 67.24, 66.34, 65.49, 61.22, 61.19, 58.43, 56.19, 51.94, 51.18, 14.53.

**(S)-4-(((R)-6-(2-Bromo-4-fluorophenyl)-5-(ethoxycarbonyl)-2-(thiazol-2-yl)-3,6-dihydropyrimidin-4-yl)methyl)morpholine-3-carboxylic Acid ((R)-53)**. HRMS: calcd (M) 552.0478, exptl (MH<sup>+</sup>) 553.0585.  $^1\text{H}$  NMR (600 MHz, methanol- $d_4$ )  $\delta$  8.11 (d,  $J = 3.0$  Hz, 1H), 8.06 (d,  $J = 3.0$  Hz, 1H), 7.67 (dd,  $J = 8.7, 5.9$  Hz, 1H), 7.51 (dd,  $J = 8.4, 2.5$  Hz, 1H), 7.22 (td,  $J = 8.4, 2.5$  Hz, 1H), 6.29 (s, 1H), 4.65 (d,  $J = 16.2$  Hz, 1H), 4.38 (t,  $J = 4.1$  Hz, 1H), 4.30–4.19 (m, 3H), 4.16–4.10 (m, 2H), 4.08–3.98 (m, 2H), 3.89–3.82 (m, 1H), 3.40–3.34 (m, 1H), 1.16 (t,  $J = 7.1$  Hz, 3H).  $^{13}\text{C}$  NMR (100 MHz, methanol- $d_4$ )  $\delta$  170.12, 168.39, 165.70, 164.97, 162.47, 158.91, 151.71, 146.23, 146.15, 139.16, 139.12, 133.62, 133.53, 128.19, 123.94, 123.84, 121.50, 121.25, 116.94, 116.72, 108.83, 66.99, 66.54, 64.96, 64.57, 63.25, 62.23, 58.32, 56.04, 55.95, 54.64, 51.76, 14.39.

**Ethyl 4-(2-Bromo-4-fluorophenyl)-6-(((R)-3-(hydroxymethyl)morpholino)methyl)-2-(thiazol-2-yl)-1,4-dihydropyrimidine-5-carboxylate (54).** HRMS: calcd (M) 538.0686, exptl (MH<sup>+</sup>) 539.0734. <sup>1</sup>H NMR (600 MHz, methanol-*d*<sub>4</sub>) δ 7.96 (t, *J* = 3.3 Hz, 1H), 7.74 (d, *J* = 2.8 Hz, 1H), 7.49–7.37 (m, 2H), 7.09 (t, *J* = 7.9 Hz, 1H), 6.16 (d, *J* = 2.9 Hz, 1H), 4.48–4.45 (m, 1H), 4.14–3.98 (m, 3H), 3.96–3.91 (m, 1H), 3.88–3.69 (m, 4H), 3.68–3.62 (m, 1H), 2.93–2.77 (m, 1H), 2.73–2.65 (m, 1H), 2.64–2.53 (m, 1H), 1.15 (t, *J* = 7.1 Hz, 3H). <sup>13</sup>C NMR (150 MHz, methanol-*d*<sub>4</sub>) δ 166.10, 166.08, 162.32, 162.07, 160.67, 147.69, 147.37, 144.99, 143.22, 140.16, 140.13, 140.06, 140.04, 130.83, 130.77, 130.70, 123.60, 123.58, 119.54, 119.50, 119.37, 119.33, 114.80, 114.66, 97.48, 96.94, 68.78, 68.76, 66.74, 66.67, 61.74, 61.24, 59.63, 59.45, 59.06, 58.49, 58.43, 53.65, 52.91, 51.93, 51.80, 13.17.

**(2R,3S)-4-(((R)-6-(2-Bromo-4-fluorophenyl)-5-(ethoxycarbonyl)-2-(thiazol-2-yl)-3,6-dihydropyrimidin-4-yl)methyl)-2-methylmorpholine-3-carboxylic Acid (55).** HRMS: calcd (M) 566.0635, exptl (MH<sup>+</sup>) 567.0724. <sup>1</sup>H NMR (600 MHz, methanol-*d*<sub>4</sub>) δ 7.97 (d, *J* = 3.0 Hz, 1H), 7.78 (d, *J* = 2.6 Hz, 1H), 7.47–7.42 (m, 2H), 7.13 (td, *J* = 8.4, 2.1 Hz, 1H), 6.15 (s, 1H), 4.36 (d, *J* = 16.6 Hz, 1H), 4.07–4.02 (m, 4H), 3.90–3.83 (m, 2H), 3.25 (s, 2H), 2.90 (s, 1H), 1.34 (d, *J* = 6.2 Hz, 3H), 1.14 (t, *J* = 7.1 Hz, 3H). <sup>13</sup>C NMR (150 MHz, methanol-*d*<sub>4</sub>) δ 171.58, 165.58, 162.52, 161.67, 160.86, 146.99, 143.65, 139.77, 131.15, 131.09, 124.05, 122.55, 122.49, 119.65, 119.49, 115.0, 114.85, 109.99, 73.90, 71.95, 65.07, 59.92, 55.70, 51.28, 17.29, 13.11.

**(3S)-4-(((R)-6-(2-Bromo-4-fluorophenyl)-5-(ethoxycarbonyl)-2-(thiazol-2-yl)-3,6-dihydropyrimidin-4-yl)methyl)-6,6-dimethylmorpholine-3-carboxylic Acid (56).** HRMS: calcd (M) 580.0791, exptl (MH<sup>+</sup>) 581.0873. <sup>1</sup>H NMR (600 MHz, methanol-*d*<sub>4</sub>) δ 7.93 (d, *J* = 3.1 Hz, 1H), 7.76 (d, *J* = 3.0 Hz, 1H), 7.49–7.47 (m, 1H), 7.41 (dd, *J* = 8.4, 2.6 Hz, 1H), 7.11 (td, *J* = 8.4, 2.5 Hz, 1H), 6.17 (s, 1H), 4.35 (d, *J* = 17.2 Hz, 1H), 4.14–3.99 (m, 5H), 3.49 (s, 1H), 3.00 (d, *J* = 11.5 Hz, 1H), 2.54–2.48 (m, 1H), 1.36 (s, 3H), 1.33 (s, 3H), 1.15 (t, *J* = 7.1 Hz, 3H). <sup>13</sup>C NMR (100 MHz, methanol-*d*<sub>4</sub>) δ 175.16, 167.03, 164.30, 163.09, 161.82, 147.93, 144.92, 141.05, 141.02, 132.48, 132.44, 132.39, 132.35, 125.54, 125.51, 123.99, 123.97, 123.90, 123.87, 121.07, 120.82, 116.42, 116.40, 116.21, 116.19, 111.37, 75.59, 75.33, 66.26, 66.05, 61.51, 61.34, 57.97, 56.07, 55.82, 53.92, 53.72, 14.51.

**(S)-1-(((R)-6-(2-Bromo-4-fluorophenyl)-5-(ethoxycarbonyl)-2-(thiazol-2-yl)-3,6-dihydropyrimidin-4-yl)methyl)-4,4-difluoropyrrolidine-2-carboxylic Acid (57).** HRMS: calcd (M) 572.0341, exptl (MH<sup>+</sup>) 573.0399. <sup>1</sup>H NMR (400 MHz, methanol-*d*<sub>4</sub>) δ 7.92 (d, *J* = 2.9 Hz, 1H), 7.73 (d, *J* = 2.9 Hz, 1H), 7.48–7.40 (m, 2H), 7.17–7.07 (m, 1H), 6.15 (s, 1H), 4.45 (d, *J* = 16.3 Hz, 1H), 4.20 (d, *J* = 16.3 Hz, 1H), 4.05 (q, *J* = 7.1 Hz, 2H), 3.96 (t, *J* = 7.9 Hz, 1H), 3.66 (q, *J* = 11.3 Hz, 1H), 3.24 (q, 11.3 Hz, 1H), 2.89–2.72 (m, 1H), 2.65–2.52 (m, 1H), 1.14 (t, *J* = 7.1 Hz, 3H). <sup>13</sup>C NMR (150 MHz, methanol-*d*<sub>4</sub>) δ 174.51, 167.22, 163.81, 163.15, 162.16, 148.62, 147.38, 144.75, 141.33, 141.31, 132.34, 132.28, 130.57, 128.93, 127.29, 125.11, 124.06, 123.99, 120.98, 120.82, 116.32, 116.18, 64.99, 61.83, 61.63, 61.44, 61.24, 58.77, 53.86, 40.35, 40.18, 40.01, 14.51.

**General Procedures for the Synthesis of 3-(((R)-4-(((R)-6-(2-Bromo-4-fluorophenyl)-5-(ethoxycarbonyl)-2-(thiazol-2-yl)-3,6-dihydropyrimidin-4-yl)methyl)morpholin-2-yl)propanoic Acid (58).** (R)-*S*-1-Isopropoxy-1-oxopropan-2-yl 4-(2-Bromo-4-fluorophenyl)-6-methyl-2-(thiazol-2-yl)-1,4-dihydropyrimidine-5-carboxylate ((R)-58I-2). 2-Thiazolecarboxamide hydrochloride (1.64 g, 0.01 mol), 2-bromo-4-fluorobenzaldehyde (2.03 g, 0.01 mol), (S)-1-isopropoxy-1-oxopropan-2-yl 3-oxobutanoate (2.16 g, 0.01 mol), anhydrous sodium acetate (0.82 g, 0.01 mol), and *n*-propanol (10 mL) were added in turn to a flask. The mixture was stirred at 80 °C for 16 h. After the reaction, the mixture was cooled to 30 °C, kept at 30 °C, and stirred for 6 h. The resulting mixture was filtered. The filter cake was washed with water (330 mL) and dried in vacuo at 60 °C for 8 h to obtain the crude product (compound 58I-2). To the crude product, *n*-propanol (19.2 g) was added. The mixture was heated until the crude product dissolved completely, then it was cooled to 30 °C, kept at 30 °C, and stirred and allowed to crystallize for 3 h. The resulting mixture was filtered. The filter cake was washed with *n*-propanol (2 g) and dried in vacuo at 60 °C for 8 h to obtain the

product (compound (R)-58I-2) as a yellow solid (1.22 g, 24%). The absolute stereochemistry of (R)-58I-2 was determined by an X-ray-diffraction study (see the Supporting Information).

$$[\alpha]_D^{25} = -39.26 \quad (c = 0.2955 \text{ g/100 mL, MeOH})$$

MS (ESI, positive ion) *m/z*: 510.0 [M + H]<sup>+</sup>; <sup>1</sup>H NMR (600 MHz, DMSO-*d*<sub>6</sub>): δ 10.0 (s, 1H), 7.97 (d, 1H), 7.90 (d, 1H), 7.54 (dd, 1H), 7.37 (dd, 1H), 7.25 (td, 1H), 5.99 (s, 1H), 4.83–4.76 (m, 2H), 2.49 (s, 3H), 1.32 (d, 3H), 1.04–1.02 (m, 6H).

(R)-Ethyl 4-(2-Bromo-4-fluorophenyl)-6-methyl-2-(thiazol-2-yl)-1,4-dihydropyrimidine-5-carboxylate (58I-3). Anhydrous ethanol (44.6 g) and lithium (0.243 g, 0.035 mol) were added to a flask in turn. The mixture was stirred at 43 °C until the lithium was consumed entirely, and then a solution of (R)-58I-2 (5.1 g, 0.01 mol) in ethanol (44.6 g) was added. The reaction mixture was allowed to warm to 78 °C and was stirred for 1.5 h under a nitrogen atmosphere. After the reaction, the reaction mixture was cooled to 10 °C, kept at 10 °C, and stirred for 8 h. The mixture was filtered. The filtrate was washed with anhydrous ethanol (5 g) and water (50 g) in turn, and then dried in vacuo at 60 °C for 8 h to obtain the product (compound 58I-3) as a yellow solid (2.97 g, 70%).

$$[\alpha]_D^{25} = -80.71 \quad (c = 0.3023 \text{ g/100 mL, MeOH})$$

MS (ESI, positive ion) *m/z*: 424.0 [M + H]<sup>+</sup>; <sup>1</sup>H NMR (400 MHz, DMSO-*d*<sub>6</sub>): δ 9.88 (s, 1H), 7.97 (d, 1H), 7.89 (d, 1H), 7.54 (dd, 1H), 7.35 (dd, 1H), 7.23 (td, 1H), 5.96 (s, 1H), 3.93 (q, 2H), 2.46 (s, 3H), 1.03 (t, 3H).

(R)-Ethyl 4-(2-Bromo-4-fluorophenyl)-6-(bromomethyl)-2-(thiazol-2-yl)-1,4-dihydropyrimidine-5-carboxylate (58I-4). (R)-Ethyl 4-(2-bromo-4-fluorophenyl)-6-methyl-2-(thiazol-2-yl)-1,4-dihydropyrimidine-5-carboxylate (compound 58I-3, 4.24 g, 0.01 mol) and CCl<sub>4</sub> (80 mL), followed by NBS (1.96 g, 0.011 mol), were added to a flask at 70 °C. The mixture was stirred for 30 min. After the reaction, the mixture was cooled and filtered. The filtrate was concentrated to obtain the product (compound 58I-4) as a yellow solid (3.42 g, 68%).

MS (ESI, positive ion) *m/z*: 503.9 [M + H]<sup>+</sup>; <sup>1</sup>H NMR (600 MHz, DMSO-*d*<sub>6</sub>): δ 10.23 (s, 1H), 8.01 (d, 1H), 7.98 (d, 1H), 7.62 (dd, 1H), 7.42 (dd, 1H), 7.29 (td, 1H), 6.01 (s, 1H), 4.79 (br, 2H), 4.01 (q, 2H), 1.08 (t, 3H).

3-(((R)-4-(((R)-6-(2-Bromo-4-fluorophenyl)-5-(ethoxycarbonyl)-2-(thiazol-2-yl)-3,6-dihydropyrimidin-4-yl)methyl)morpholin-2-yl)propanoic Acid (58). (R)-Ethyl 4-(2-bromo-4-fluorophenyl)-6-(bromomethyl)-2-(thiazol-2-yl)-1,4-dihydropyrimidine-5-carboxylate (compound 58I-4, 0.05 g, 0.001 mol), anhydrous ethanol (10 g), and (R)-3-(morpholin-2-yl)propanoic acid (0.175 g, 0.0011 mol) were added to a flask. The mixture was stirred at 25 °C under a nitrogen atmosphere for 6 h. After the reaction, the mixture was concentrated. Ethyl acetate (10 g) was added to the residue, and the resulting mixture was washed with water (15 mL × 2). The organic layer was concentrated to give 3-(((R)-4-(((R)-6-(2-bromo-4-fluorophenyl)-5-(ethoxycarbonyl)-2-(thiazol-2-yl)-3,6-dihydropyrimidin-4-yl)methyl)morpholin-2-yl)propanoic acid (compound 58) as tawny oil (0.38 g, 65%). HRMS: calcd (M) 580.0791, exptl (MH<sup>+</sup>) 581.086. <sup>1</sup>H NMR (600 MHz, DMSO-*d*<sub>6</sub>) δ 12.04 (s, 1H), 9.65 (s, 1H), 8.02 (d, *J* = 3.1 Hz, 1H), 7.94 (d, *J* = 3.1 Hz, 1H), 7.56 (dd, *J* = 8.5, 2.6 Hz, 1H), 7.40–7.38 (m, 1H), 7.22 (td, *J* = 8.5, 2.6 Hz, 1H), 6.03 (s, 1H), 3.99–3.92 (m, 2H), 3.90–3.87 (m, 3H), 3.58 (td, *J* = 11.2, 1.9 Hz, 1H), 3.53–3.47 (m, 1H), 2.80–2.75 (m, 2H), 2.35 (td, *J* = 11.4, 3.0 Hz, 1H), 2.31–2.23 (m, 2H), 2.02 (t, *J* = 10.5 Hz, 1H), 1.69–1.56 (m, 2H), 1.06 (t, *J* = 7.1 Hz, 3H). <sup>13</sup>C NMR (150 MHz, DMSO-*d*<sub>6</sub>) δ 174.69, 165.64, 162.46, 162.07, 160.42, 146.84, 144.36, 144.09, 140.70, 140.68, 131.41, 131.35, 125.14, 123.08, 123.01, 120.14, 119.98, 116.03, 115.89, 97.59, 74.92, 66.54, 59.86, 58.66, 58.29, 56.26, 53.26, 29.98, 28.52, 14.46.

3-(((S)-4-(((R)-6-(2-Bromo-4-fluorophenyl)-5-(ethoxycarbonyl)-2-(thiazol-2-yl)-3,6-dihydropyrimidin-4-yl)methyl)morpholin-2-yl)propanoic Acid (59). HRMS: calcd (M) 580.0791, exptl (MH<sup>+</sup>) 581.0862. <sup>1</sup>H NMR (600 MHz, acetone-*d*<sub>6</sub>) δ 9.72 (s, 1H), 7.97 (d, *J* = 3.1 Hz, 1H), 7.80 (d, *J* = 3.0 Hz, 1H), 7.55–7.49 (m, 1H), 7.44 (dd, *J* = 8.5, 2.6 Hz, 1H), 7.13 (td, *J* = 8.4, 2.5 Hz, 1H), 6.19

(s, 1H), 4.09 (d,  $J = 16.8$  Hz, 1H), 4.03 (q,  $J = 7.1$  Hz, 2H), 3.95 (d,  $J = 16.6$  Hz, 1H), 3.90 (d,  $J = 11.1$  Hz, 1H), 3.74–3.68 (m, 2H), 2.98 (d,  $J = 8.6$  Hz, 1H), 2.74 (d,  $J = 7.3$  Hz, 1H), 2.54–2.41 (m, 3H), 2.37 (s, 1H), 2.29–2.20 (m, 1H), 1.83–1.78 (m, 2H), 1.13 (t,  $J = 7.1$  Hz, 3H).  $^{13}\text{C}$  NMR (150 MHz, acetone- $d_6$ )  $\delta$  173.66, 165.38, 162.77, 162.16, 160.51, 146.47, 144.28, 143.46, 140.59, 131.17, 131.12, 123.77, 122.92, 122.86, 119.65, 119.49, 115.15, 115.01, 97.80, 74.81, 66.37, 59.38, 58.72, 58.45, 56.30, 53.01, 13.64.

**3-((3S)-4-(((R)-6-(2-Bromo-4-fluorophenyl)-5-(ethoxycarbonyl)-2-(thiazol-2-yl)-3,6-dihydropyrimidin-4-yl)methyl)morpholin-3-yl)propanoic Acid (60).** HRMS: calcd (M) 580.0791, exptl (MH<sup>+</sup>) 581.086.  $^1\text{H}$  NMR (600 MHz, acetone- $d_6$ )  $\delta$  9.93 (s, 1H), 7.98 (d,  $J = 3.1$  Hz, 1H), 7.80 (d,  $J = 3.1$  Hz, 1H), 7.54–7.51 (m, 1H), 7.42 (dd,  $J = 8.5, 2.6$  Hz, 1H), 7.16 (td,  $J = 8.5, 2.6$  Hz, 1H), 6.18 (s, 1H), 4.33 (d,  $J = 18.0$  Hz, 1H), 4.04–4.01 (m, 3H), 3.93 (dd,  $J = 11.4, 2.7$  Hz, 1H), 3.83–3.80 (m, 1H), 3.77–3.70 (m, 1H), 3.51–3.47 (m, 1H), 3.01 (s, 1H), 2.90 (d,  $J = 10.8$  Hz, 1H), 2.70–2.60 (m, 2H), 2.51–2.46 (m, 1H), 2.44–2.37 (m, 1H), 1.86–1.78 (m, 1H), 1.13 (t,  $J = 7.1$  Hz, 3H).  $^{13}\text{C}$  NMR (150 MHz, acetone- $d_6$ )  $\delta$  173.65, 165.47, 162.80, 162.12, 160.48, 147.69, 144.26, 143.50, 140.66, 131.30, 131.24, 123.79, 122.83, 122.77, 119.55, 119.39, 115.36, 115.22, 96.47, 70.04, 66.75, 59.81, 59.33, 58.64, 53.46, 52.40, 13.66.

**3-((3R)-4-(((R)-6-(2-Bromo-4-fluorophenyl)-5-(ethoxycarbonyl)-2-(thiazol-2-yl)-3,6-dihydropyrimidin-4-yl)methyl)morpholin-3-yl)propanoic Acid (61).** HRMS: calcd (M) 580.0791, exptl (MH<sup>+</sup>) 581.0862.  $^1\text{H}$  NMR (600 MHz, acetone- $d_6$ )  $\delta$  9.93 (s, 1H), 7.99 (d,  $J = 3.1$  Hz, 1H), 7.79 (d,  $J = 3.1$  Hz, 1H), 7.52–7.49 (m, 1H), 7.43 (dd,  $J = 8.5, 2.6$  Hz, 1H), 7.11 (td,  $J = 8.4, 2.6$  Hz, 1H), 6.18 (s, 1H), 4.37 (d,  $J = 17.9$  Hz, 1H), 4.05–4.01 (m, 3H), 3.89 (dd,  $J = 11.4, 2.7$  Hz, 1H), 3.81–3.80 (m, 1H), 3.76–3.70 (m, 1H), 3.58–3.55 (m, 1H), 2.99–2.96 (m, 1H), 2.72–2.69 (m, 1H), 2.63–2.55 (m, 1H), 2.48–2.35 (m, 2H), 2.00–1.94 (m, 1H), 1.86–1.80 (m, 1H), 1.13 (t,  $J = 7.1$  Hz, 3H).  $^{13}\text{C}$  NMR (150 MHz, acetone- $d_6$ )  $\delta$  173.51, 165.44, 162.86, 162.12, 160.48, 147.66, 147.59, 144.25, 143.48, 140.67, 131.19, 131.13, 123.73, 122.94, 122.88, 119.63, 119.47, 115.11, 114.97, 96.52, 69.62, 66.66, 59.32, 59.29, 58.81, 53.35, 51.28, 13.66.

**(3S)-4-(((R)-6-(2-Bromo-4-fluorophenyl)-5-(ethoxycarbonyl)-2-(1-methyl-1H-imidazol-2-yl)-3,6-dihydropyrimidin-4-yl)methyl)morpholine-3-carboxylic Acid (62).** The synthetic procedure was described in the Supporting Information. HRMS: calcd (M) 549.1023, exptl (MH<sup>+</sup>) 550.1090.  $^1\text{H}$  NMR (600 MHz, acetone- $d_6$ )  $\delta$  7.46–7.43 (m, 1H), 7.42–7.39 (m, 1H), 7.21 (d,  $J = 4.5$  Hz, 1H), 7.11–7.07 (m, 1H), 7.03 (s, 1H), 6.17 (d,  $J = 8.8$  Hz, 1H), 4.34 (d,  $J = 17.7$  Hz, 1H), 4.22 (d,  $J = 17.7$  Hz, 1H), 4.18–4.11 (m, 1H), 4.05–4.01 (m, 3H), 3.99 (d,  $J = 7.2$  Hz, 3H), 3.88–3.76 (m, 2H), 3.67–3.54 (m, 1H), 3.26–3.21 (m, 1H), 2.62–2.44 (m, 1H), 1.13 (t,  $J = 7.1$  Hz, 3H).  $^{13}\text{C}$  NMR (150 MHz, acetone- $d_6$ )  $\delta$  171.71, 165.55, 165.54, 162.05, 160.41, 148.22, 143.00, 140.18, 140.16, 140.06, 140.04, 138.71, 138.69, 130.31, 130.25, 127.55, 127.54, 125.94, 125.92, 123.10, 123.05, 123.03, 119.86, 119.84, 119.69, 119.68, 114.76, 114.72, 114.63, 114.59, 95.59, 95.33, 69.22, 69.13, 67.04, 66.99, 62.12, 59.18, 58.16, 58.11, 54.79, 49.31, 48.37, 35.50, 13.68.

**3-(((R)-4-(((R)-6-(2-Bromo-4-fluorophenyl)-5-(methoxycarbonyl)-2-(thiazol-2-yl)-3,6-dihydropyrimidin-4-yl)methyl)morpholin-2-yl)propanoic Acid (63).** HRMS: calcd (M) 566.0635, exptl (MH<sup>+</sup>) 567.0707.  $^1\text{H}$  NMR (600 MHz, acetone- $d_6$ )  $\delta$  9.76 (s, 1H), 7.97 (d,  $J = 3.1$  Hz, 1H), 7.79 (d,  $J = 3.1$  Hz, 1H), 7.49–7.47 (m, 1H), 7.44 (dd,  $J = 8.5, 2.6$  Hz, 1H), 7.11 (td,  $J = 8.4, 2.6$  Hz, 1H), 6.17 (s, 1H), 4.00 (q,  $J = 17.2$  Hz, 2H), 3.96–3.92 (m, 1H), 3.73 (td,  $J = 11.3, 2.3$  Hz, 1H), 3.69–3.65 (m, 1H), 3.58 (s, 3H), 2.89–2.84 (m, 2H), 2.50–2.37 (m, 3H), 2.13 (t,  $J = 10.5$  Hz, 1H), 1.77–1.74 (m, 2H).  $^{13}\text{C}$  NMR (150 MHz, acetone- $d_6$ )  $\delta$  173.56, 165.88, 162.73, 162.67, 162.16, 160.51, 146.77, 146.69, 144.40, 144.36, 143.49, 140.31, 140.29, 130.99, 130.94, 123.74, 122.99, 122.92, 119.79, 119.63, 115.10, 114.96, 97.27, 74.81, 66.47, 58.66, 58.28, 56.44, 56.41, 53.24, 50.35.

**3-((R)-4-(((R)-6-(2-Chloro-4-fluorophenyl)-5-(methoxycarbonyl)-2-(thiazol-2-yl)-3,6-dihydropyrimidin-4-yl)methyl)morpholin-2-yl)propanoic Acid (64).** HRMS: calcd (M) 522.1140, exptl (MH<sup>+</sup>) 523.1240.  $^1\text{H}$  NMR (400 MHz, methanol- $d_4$ )  $\delta$  7.96 (d,  $J = 3.0$  Hz, 1H), 7.75 (d,  $J = 3.0$  Hz, 1H), 7.43–7.39 (m, 1H), 7.23 (dd,  $J = 8.7, 2.3$  Hz, 1H), 7.05 (td,  $J = 8.4, 2.3$  Hz, 1H), 6.17 (s, 1H), 4.09–

3.90 (m, 3H), 3.79 (t,  $J = 10.5$  Hz, 1H), 3.73–3.68 (m, 1H), 3.61 (s, 2H), 2.93–2.77 (m, 2H), 2.55 (t,  $J = 10.1$  Hz, 1H), 2.47–2.33 (m, 2H), 2.17 (t,  $J = 9.5$  Hz, 1H), 1.76 (q,  $J = 7.1$  Hz, 2H).  $^{13}\text{C}$  NMR (101 MHz, methanol- $d_4$ )  $\delta$  175.91, 166.37, 162.94, 161.82, 160.47, 146.79, 145.70, 143.37, 137.88, 137.85, 133.46, 133.36, 130.82, 130.73, 123.72, 116.55, 116.30, 114.27, 114.05, 98.21, 74.84, 66.20, 57.98, 56.39, 55.69, 53.02, 50.25, 29.54.

**3-(((R)-4-(((R)-6-(2,4-Dichlorophenyl)-5-(methoxycarbonyl)-2-(thiazol-2-yl)-3,6-dihydropyrimidin-4-yl)methyl)morpholin-2-yl)propanoic Acid (65).** HRMS: calcd (M) 538.0844, exptl (MH<sup>+</sup>) 539.0488.  $^1\text{H}$  NMR (600 MHz, acetone- $d_6$ )  $\delta$  9.78 (s, 1H), 7.97 (d,  $J = 3.1$  Hz, 1H), 7.79 (d,  $J = 3.1$  Hz, 1H), 7.49 (d,  $J = 2.1$  Hz, 1H), 7.46 (q,  $J = 8.4$  Hz, 1H), 7.31 (dd,  $J = 8.4, 2.0$  Hz, 1H), 6.19 (s, 1H), 4.00 (d,  $J = 17.2$  Hz, 2H), 3.95–3.92 (m, 1H), 3.73 (td,  $J = 11.1, 2.2$  Hz, 1H), 3.75–3.71 (m, 1H), 3.58 (s, 3H), 2.86 (t,  $J = 12.6$  Hz, 2H), 2.50–2.37 (m, 3H), 2.13 (t,  $J = 10.5$  Hz, 1H), 1.77–1.74 (dd,  $J = 14.1, 7.4$  Hz, 2H).  $^{13}\text{C}$  NMR (150 MHz, acetone- $d_6$ )  $\delta$  173.54, 165.80, 162.59, 146.87, 144.63, 143.51, 141.15, 133.52, 133.00, 130.99, 129.07, 127.69, 123.79, 96.72, 74.80, 66.46, 58.28, 56.51, 56.42, 53.24, 50.38.

**3-(((S)-1-(((R)-6-(2-Bromo-4-fluorophenyl)-5-(ethoxycarbonyl)-2-(thiazol-2-yl)-3,6-dihydropyrimidin-4-yl)methyl)-4,4-difluoropyrrolidin-2-yl)propanoic Acid (66).** The synthetic procedure was described in the Supporting Information. HRMS: calcd (M) 600.0654, exptl (MH<sup>+</sup>) 601.0723.  $^1\text{H}$  NMR (600 MHz, acetone)  $\delta$  7.95 (d,  $J = 3.1$  Hz, 1H), 7.81 (d,  $J = 3.1$  Hz, 1H), 7.59–7.56 (m, 1H), 7.44 (dd,  $J = 8.5, 2.6$  Hz, 1H), 7.16 (td,  $J = 8.5, 2.6$  Hz, 1H), 6.19 (s, 1H), 4.29 (q,  $J = 17.1$  Hz, 2H), 4.03 (q,  $J = 7.1$  Hz, 2H), 3.64–3.59 (m, 1H), 3.25–3.21 (m, 1H), 3.10–3.02 (m, 1H), 2.70–2.59 (m, 1H), 2.58–2.50 (m, 1H), 2.49–2.41 (m, 1H), 2.28–2.16 (m, 2H), 1.93–1.86 (m, 1H), 1.12 (t,  $J = 7.1$  Hz, 3H).  $^{13}\text{C}$  NMR (150 MHz, acetone- $d_6$ )  $\delta$  173.78, 165.37, 162.73, 162.19, 160.54, 147.13, 144.38, 143.44, 140.64, 140.61, 131.40, 131.35, 129.81, 128.19, 126.54, 123.96, 122.77, 122.71, 119.57, 119.41, 115.34, 115.20, 97.99, 63.21, 63.18, 62.10, 61.91, 61.71, 59.46, 58.15, 51.84, 40.60, 40.44, 40.28, 29.27, 27.73, 13.60.

**Molecular Docking.** For docking purposes, the crystallographic coordinates of the HBcAg (PDB ID SE01) were obtained from the protein data bank ([www.rcsb.org](http://www.rcsb.org)). Hydrogen atoms were added to the structure to allow for appropriate ionization at physiological pH. The protonated state of several important residues, such as His106, His142, Tyr599, Glu751, and His640, were adjusted by using SYBYL7.3 (Tripos, St. Louis, MO) to favor the formation of reasonable hydrogen bonds with the ligand. Molecular-docking analysis was carried out by the SURFLEX module of the SYBYL package in order to explore the interaction model for the active site of HBcAg with its ligand. All atoms located within the range of 6.0 Å from any atom of the original ligand were selected for the active-site analysis, and the corresponding amino acid residue was, therefore, involved in the active-site analysis even if only one of its atoms was selected. Other default parameters were adopted in the SURFLEX-docking calculations. All calculations were performed on a CCNU Grid based computational environment (CCNU Grid website: <http://www.202.114.32.71:8090/ccnu/chem/platform.xml>).

**In Vitro Biological Testing. General Considerations.** All final compounds were examined for known classes of assay-interference compounds (pan assay-interference compounds, PAINS),<sup>32</sup> which were classified as negative.

**In Vitro Anti-HBV Activity in HepG2.2.15.** HBV replicon cells, HepG2.2.15, were seeded into 96-well plates at  $4 \times 10^5$  cells/well, treated with cell-culture medium (RPMI 1640 containing 10% FBS, 2 mM L-glutamine, 100 units/mL penicillin, and 10  $\mu\text{g}/\text{mL}$  streptomycin), and incubated overnight at 37 °C. The control and test compounds were 3-fold diluted with medium and added into the plates with a 0.5% final DMSO concentration. The plates were then incubated at 37 °C in a 5% carbon dioxide atmosphere and refreshed with compound-containing medium every 3 days. On day 7, the HepG2.2.15 supernatant was collected and HBV DNA was extracted using the QIAamp 96 DNA Blood Kit (QIAGEN 51161, Hilden, Germany). The HBV DNA was quantified by real-time PCR. The primers and probe used were as follows:

HBV forward primer: 5'-GTGTCTGCGGGCGTTTATCA-3'

HBV reverse primer: 5'-GACAAACGGGCAACATACCTT-3'

HBV probe: 5'-FAM-CCTCTKCATCCTGCTGCTAT-GCCTCATC-3'

A standard curve was generated by plotting Ct value versus the amount of the HBV-plasmid standard, and the quantity of each sample was estimated on the basis of the Ct-value projection on the standard curve; the percent of HBV inhibition by compound was calculated using the following equation:

$$\text{inh\%} = (1 - \text{sample HBV quantity} / \text{DMSO-control HBV quantity}) \times 100\%$$

The EC<sub>50</sub> were plotted with GraphPad Prism 4 using the equation below.

$$\text{sigmoidal dose-response (variable slope), } Y = \text{bottom} + (\text{top} - \text{bottom}) / (1 + 10^{(\log EC_{50} - X) \times \text{hill slope}})$$

where X is the logarithm of the concentration, and Y is the response. Y starts at the bottom and goes to the top with a sigmoid shape. This is identical to the "four parameter logistic equation".

**hERG assay.** In vitro electrophysiology manual-patch-clamp assays of selected compounds on hERG channels were conducted in PharmaCore Laboratories, Ltd. (Jiangsu, China) in compliance with their Standard Operating Procedures. In detail, HEK293 cells were perfused with an extracellular solution, and membrane currents were recorded by a HEKA EPC-10 USB patch-clamp amplifier and a PATCHMASTER acquisition program (HEKA Instruments Inc., Lambrecht, Germany) at room temperature. The electrophysiological-voltage protocol for the hERG-current recordings was the following: Cells were voltage clamped at a holding potential of -80 mV. The hERG current was activated by depolarizing at +20 mV for 2 s, after which the current was taken back to -50 mV for 5 s to remove the inactivation and observe the deactivating tail current. The stimulation frequency was once every 15 s. The current amplitude was the peak value of the tail current. The channel current was recorded in the whole-cell recording mode. The extracellular fluid was perfused and recorded continuously until stabilization. Then, the extracellular fluid containing the tested compound was perfused and recorded until the inhibition of the hERG current reached a steady state. Data were analyzed using PATCHMASTER V2 × 60 (HEKA Instruments Inc., Lambrecht, Germany) and Origin 8.5 (OriginLab Corporation, Northampton, MA) software programs and Microsoft Excel.

**Microsomal-Stability Assay.** Microsomes were preincubated with a test compound for 10 min at 37 °C in 100 mM potassium phosphate buffer (pH 7.4). The reactions were initiated by adding NADPH to give a final incubation volume of 45 μL. The incubations contained 1 μM test compound, 0.5 mg/mL liver microsomal protein, and 2 mM NADPH in 100 mM potassium phosphate buffer (pH 7.4). After incubation times of 0, 15, 30, and 60 min at 37 °C, stop solution was added (150 μL/well) to terminate the reaction. Following precipitation and centrifugation, the amounts of compound remaining in the samples were determined by LC-MS/MS.

**Cytochrome-P450 (Cyp450)-Induction-Screening Assay: Enzyme-Activity Induction.** Cryopreserved hepatocytes were thawed and counted to determine their yield, and their viability was measured. Hepatocytes at a concentration of 0.7 million cells/mL were transferred to collagen-coated 48-well plates for attachment (0.2 mL viable cells/well). After the hepatocytes attached to the collagen matrix, the plating medium was replaced with an incubation medium containing 2% (v/v) Matrigel (sandwich medium), and the hepatocytes were incubated until their use. All incubations were conducted at 37 °C, 5% CO<sub>2</sub>, and 95% humidity.

After the cultures were established, the sandwich medium was removed and the hepatocytes were treated for 24 h with incubation solutions that contained a vehicle (0.1% DMSO) and a test compound or were a negative control or a positive control. The incubation solution was aspirated and replaced the appropriate fresh solution for

an additional 24 h incubation. The total treatment period was 48 h. After the treatment period of 48 h, the incubation solution was aspirated. Hepatocytes were washed twice with HBSS, followed by the addition of the enzyme-substrate working solution. The hepatocytes were incubated for 30 min.

After the incubation, 75 μL of the samples were aspirated and quenched with 150 μL of the stop solution. The resulting mixtures were shaken for 10 min, which was followed by centrifugation at 4 °C and 3220g for 20 min. For each, an aliquot of the supernatant were mixed with 0.1% FA in water at a ratio of 1:4. The resulting samples were shaken for 10 min prior to analysis by LC-MS/MS. The concentrations of the three metabolites of the CYP-enzyme substrate, 1'-hydroxymidazolam, hydroxybupropion, and acetaminophen, in the human hepatocytes were quantitatively determined by LC-MS/MS after the proteins were precipitated.

**In Vivo Efficacy in the Hydrodynamic-Injection (HDI) Mouse Model.** This study was conducted by WuXi AppTec Company, Ltd. (Shanghai, China). All the procedures in the study were in compliance with local animal-welfare legislation, the Guide for the Care and Use of Laboratory Animals, and protocols approved by the WuXi AppTec Institutional Animal Care and Use Committee (IACUC).

Female BALB/c mice (6–7 weeks old, 16–18 g) that were specific-pathogen free were supplied by Shanghai Lingchang Biotechnology Company, Ltd. (Shanghai, China). The study was approved by the WuXi IACUC (IACUC protocol R20160125-Mouse). On day 0, all the mice were hydrodynamically injected with pAAV2-HBV1.3mer plasmid DNA (genotype D) in a volume of normal saline equivalent to 8% of a mouse's body weight within 5 s through a tail vein. From days 1 to 7, the mice in all the groups were orally dosed with the blank vehicle, 0.1 mg/kg entecavir, 50 mg/kg HEC72702, or 100 mg/kg HEC72702 at the indicated frequency. Plasma and liver samples were collected at the indicated time points for HBV-DNA quantification by real-time PCR.

**Pharmacokinetic (PK) Analysis.** All pharmacokinetic studies in male Sprague–Dawley (SD) rats and beagle dogs were conducted according to protocols approved by the Animal Care and Use Committee at the Laboratory Animal Center of HEC Pharma Group. Briefly, male SD rats were obtained from Hunan SJA Laboratory Animal Company, Ltd. (China) and maintained on a 12 h light–dark cycle with ad libitum access to food and water. Non-naïve beagle dogs supplied by Beijing Marshall Biotechnology Company, Ltd. (Beijing, China) were used in this study. The animals were confirmed healthy before being assigned to the study. Each animal was given a unique identification number marked on the ear and written on the cage card.

The compounds were evaluated in Sprague–Dawley rats (6–7 weeks old, 190–240 g), which had fasted overnight before their dosings, and their food was returned 4 h after their dosings. There were three rats in the iv group and three rats in the po group, all of which had blood samples taken (iv group, 1 mg/kg; po group, 5 mg/kg). The compounds were dissolved in 5% DMSO, 5% solutol, and 90% saline for iv and po doses. Blood samples were collected at each time point, placed into tubes containing sodium heparin, and centrifuged at 12 000 rpm for 2 min at 4 °C to separate the plasma from the samples. Following centrifugation, the resulting plasma was transferred to clean tubes and stored frozen at -80 °C pending bioanalysis. Plasma concentrations were determined by LC-MS/MS, and the data were analyzed by a noncompartmental module of a WinNonlin 6.3. Any BLQs were omitted from the calculations.

All dogs (7–9 months old, 8–12 kg) fasted overnight before their first dosings; their food was returned immediately after the oral dosing and at 4 h post the first dosing. Reverse-osmosis (RO) water was available to all the animals, ad libitum. There were three dogs in the iv group and three dogs in the po group, all of which had blood samples taken (iv group, 1 mg/kg; po group, 5 mg/kg). The compounds were dissolved in 5% DMSO, 5% solutol, and 90% saline for the iv and po doses. Blood samples were collected at each time point, placed into tubes containing sodium heparin, and centrifuged at 12 000 rpm for 2 min at 4 °C to separate the plasma from the samples. Following centrifugation, the resulting plasma was transferred to clean tubes and stored frozen at -80 °C pending bioanalysis. Plasma concentrations

were determined by LC-MS/MS, and the data were analyzed by a noncompartmental module of a WinNonlin 6.3. Any BLQs were omitted from the calculations.

## ■ ASSOCIATED CONTENT

### Supporting Information

The Supporting Information is available free of charge on the ACS Publications website at DOI: 10.1021/acs.jmedchem.7b01914.

Detailed experimental procedures for the synthesis of intermediates **58I-1** and analogues **35**, **62**, and **66**; characterization of compounds **6–25**; X-ray crystal structure of (**R**)-**58I-2**;  $^1\text{H}$  NMR and  $^{13}\text{C}$  NMR spectra of compound **58**; inhibition efficacy of (**R**)-**52** against four major HBV genotypes (A, B, C, and D); CYP inhibition assay; pharmacokinetic (PK) studies in mice; HBV-capsid-assembly-quenching assay (PDF) Molecular-formula strings of the reported compounds (CSV)

## ■ AUTHOR INFORMATION

### Corresponding Authors

\*Tel.: +86 18676907182, E-mail: renqingyun@hec.cn (Q.R.).

\*Tel.: +86 13925592278, E-mail: zhangyingjun@hec.cn (Y.Z.).

### ORCID

Qingyun Ren: 0000-0003-0000-0417

Siegfried Goldmann: 0000-0002-4776-0360

### Notes

The authors declare no competing financial interest.

## ■ ACKNOWLEDGMENTS

This project was supported by the National Major Scientific and Technological Special Project for "Significant New Drugs Development" during the Thirteenth Five-Year Plan Period of China (nos. 2017ZX09201006004 and 2016ZX09101065). We thank Dr. Wenchao Yang at the Central China Normal University for the molecular-docking analysis. In addition, we thank Wuxi AppTec for working together with us on the in vitro and in vivo anti-HBV-activity experiments, Shanghai Chem Explorer and Pharma Core Laboratories for the hERG-inhibition experiments, and the Research Institute for Liver Diseases (Shanghai) Company, Ltd., for the induction test on the CYP enzymes.

## ■ ABBREVIATIONS USED

HBV, hepatitis B virus; CHB, chronic hepatitis B; HAP, heteroaryl dihydropyrimidine; HBsAg, HBV surface antigen; pgRNA, pregenomic RNA; cccDNA, covalently closed circular DNA; hERG, human ether-à-go-go-related gene; ADMET, absorption, distribution, metabolism, excretion, and toxicity; HDI, hydrodynamic injection; ETV, entecavir; CYP, cytochrome P450; NBS, *N*-bromosuccinimide; PE, petroleum ether; EA, ethyl acetate; HPLC, high-performance liquid chromatography; IPA, 2-propanol; PD, pharmacodynamics; PK, pharmacokinetic; qPCR, quantitative polymerase chain reaction; q.d., once daily; b.i.d., twice daily; HLM, human liver microsome; MLM, mouse liver microsome; DLM, dog liver microsome.

## ■ REFERENCES

- (1) Ganem, D.; Prince, A. M. Hepatitis B virus infection-natural history and clinical consequences. *N. Engl. J. Med.* **2004**, *350*, 1118–1129.
- (2) Shepard, C. W.; Simard, E. P.; Finelli, L.; Fiore, A. E.; Bell, B. P. Hepatitis B virus infection: epidemiology and vaccination. *Epidemiol. Rev.* **2006**, *28*, 112–125.
- (3) Perrillo, R. Benefits and risks of interferon therapy for hepatitis B. *Hepatology* **2009**, *49*, S103–111.
- (4) Tipples, G. A.; Ma, M. M.; Fischer, K. P.; Bain, V. G.; Kneteman, N. M.; Tyrrell, D. L. Mutation in HBV RNA-dependent DNA polymerase confers resistance to lamivudine in vivo. *Hepatology* **1996**, *24*, 714–717.
- (5) Papatheodoridis, G. V.; Manolakopoulos, S.; Dusheiko, G.; Archimandritis, A. J. Therapeutic strategies in the management of patients with chronic hepatitis B virus infection. *Lancet Infect. Dis.* **2008**, *8*, 167–178.
- (6) Petersen, J.; Dandri, M.; Mier, W.; Lütgehetmann, M.; Volz, T.; von Weizsäcker, F.; Haberkorn, U.; Fischer, L.; Pollok, J.; Erbes, B.; Seitz, S.; Urban, S. Prevention of hepatitis B virus infection in vivo by entry inhibitors derived from the large envelope protein. *Nat. Biotechnol.* **2008**, *26*, 335–341.
- (7) Steven, A. C.; Conway, J. F.; Cheng, N.; Watts, N. R.; Belnap, D. M.; Harris, A.; Stahl, S. J.; Wingfield, P. T. Structure, assembly, and antigenicity of hepatitis B virus capsid proteins. *Adv. Virus Res.* **2005**, *64*, 125–164.
- (8) Chain, B. M.; Myers, R. Variability and conservation in hepatitis B virus core protein. *BMC Microbiol.* **2005**, *5*, 33.
- (9) Choi, I.-G.; Yu, Y. G. Interaction and assembly of HBV structural proteins: novel target sites of anti-HBV agents. *Infect. Disord.: Drug Targets* **2007**, *7*, 251–256.
- (10) Delaney, W. E.; Edwards, R.; Colledge, D.; Shaw, T.; Furman, P.; Painter, G.; Locarnini, S. Phenylpropenamide derivatives AT-61 and AT-130 inhibit replication of wild-type and lamivudine-resistant strains of hepatitis B virus in vitro. *Antimicrob. Agents Chemother.* **2002**, *46*, 3057–3060.
- (11) Wang, P.; Naduthambi, D.; Mosley, R. T.; Niu, C.; Furman, P. A.; Otto, M. J.; Sofia, M. J. Phenylpropenamide derivatives: antihepatitis B virus activity of the Z isomer, SAR and the search for novel analogs. *Bioorg. Med. Chem. Lett.* **2011**, *21*, 4642–4647.
- (12) Campagna, M. R.; Liu, F.; Mao, R.; Mills, C.; Cai, D.; Guo, F.; Zhao, X.; Ye, H.; Cuconati, A.; Guo, H.; Chang, J.; Xu, X.; Block, T. M.; Guo, J. T. Sulfamoylbenzamide derivatives inhibit the assembly of hepatitis B virus nucleocapsids. *J. Virol.* **2013**, *87*, 6931–6942.
- (13) Yang, L.; Shi, L. P.; Chen, H. J.; Tong, X. K.; Wang, G. F.; Zhang, Y. M.; Wang, W. L.; Feng, C. L.; He, P. L.; Zhu, F. H.; Hao, Y. H.; Wang, B. J.; Yang, D. L.; Tang, W.; Nan, F. J.; Zuo, J. P. Isothiafludine, a novel non-nucleoside compound, inhibits hepatitis B virus replication through blocking pregenomic RNA encapsidation. *Acta Pharmacol. Sin.* **2014**, *35*, 410–418.
- (14) Levin, J. NVR 3–778, a first-in-class HBV core inhibitor, alone and in combination with pegylated-interferon (peg-IFN alpha-2a), in treatment-naïve HBeAg-positive patients: early reductions in HBV DNA and HBeAg. Presented at the EASL International Liver Congress, Barcelona, April 14–17, 2016.
- (15) Levin, J. Safety, tolerability and pharmacokinetics of JNJ-56136379, a novel HBV capsid assembly modulator, in healthy subjects. Presented at the AASLD Liver Meeting, Boston, Nov 11–15, 2016.
- (16) Deres, K.; Schroder, C. H.; Paessens, A.; Goldmann, S.; Hacker, H. J.; Weber, O.; Kramer, T.; Niewohner, U.; Pleiss, U.; Stoltefuss, J.; Graef, E.; Koletzki, D.; Masantschek, R. N.; Reimann, A.; Jaeger, R.; Gross, R.; Beckermann, B.; Schlemmer, K. H.; Haebich, D.; Rubsamen-Waigmann, H. Inhibition of hepatitis B virus replication by drug-induced depletion of nucleocapsids. *Science* **2003**, *299*, 893–896.
- (17) Bourne, C. R.; Finn, M. G.; Zlotnick, A. Global structural changes in hepatitis B virus capsids induced by the assembly effector HAP1. *J. Virol.* **2006**, *80*, 11055–11061.

- (18) Brezillon, N.; Brunelle, M. N.; Massinet, H.; Giang, E.; Lamant, C.; DaSilva, L.; Berissi, S.; Belghiti, J.; Hannoun, L.; Puerstinger, G.; Wimmer, E.; Neyts, J.; Hantz, O.; Soussan, P.; Morosan, S.; Kremser, D. Antiviral activity of Bay 41–4109 on hepatitis B virus in humanized Alb-uPA/SCID mice. *PLoS One* **2011**, *6*, e25096.
- (19) Shi, C.; Wu, C. Q.; Cao, A. M.; Sheng, H. Z.; Yan, X. Z.; Liao, M. Y. NMR-spectroscopy-based metabonomic approach to the analysis of Bay41–4109, a novel anti-HBV compound, induced hepatotoxicity in rats. *Toxicol. Lett.* **2007**, *173*, 161–167.
- (20) Qiu, Z. X.; Lin, X. F.; Zhou, M. W.; Liu, Y. F.; Zhu, W.; Chen, W. M.; Zhang, W. X.; Guo, L.; Liu, H. X.; Wu, G. L.; Huang, M. W.; Jiang, M.; Xu, Z. H.; Zhou, Z.; Qin, N.; Ren, S.; Qiu, H. X.; Zhong, S.; Zhang, Y. X.; Zhang, Y.; Wu, X. Y.; Shi, L. P.; Shen, F.; Mao, Y.; Zhou, X.; Yang, W. G.; Wu, J. Z.; Yang, G.; Mayweg, A. V.; Shen, H. C.; Tang, G. Z. Design and synthesis of orally bioavailable 4-methyl heteroaryldihydropyrimidine based hepatitis B Virus (HBV) capsid inhibitors. *J. Med. Chem.* **2016**, *59*, 7651–7666.
- (21) Qiu, Z. X.; Lin, X. F.; Zhang, W. X.; Zhou, M. W.; Guo, L.; Kocer, B.; Wu, G.; Zhang, Z.; Liu, H.; Shi, H.; Kou, B.; Hu, T.; Hu, Y.; Huang, M.; Yan, S. F.; Xu, Z.; Zhou, Z.; Qin, N.; Wang, Y. F.; Ren, S.; Qiu, H.; Zhang, Y.; Zhang, Y.; Wu, X.; Sun, K.; Zhong, S.; Xie, J.; Ottaviani, G.; Zhou, Y.; Zhu, L.; Tian, X.; Shi, L.; Shen, F.; Mao, Y.; Zhou, X.; Gao, L.; Young, J. A. T.; Wu, J. Z.; Yang, G.; Mayweg, A. V.; Shen, H. C.; Tang, G.; Zhu, W. Discovery and pre-clinical characterization of third-generation 4-H heteroaryldihydropyrimidine (HAP) analogues as hepatitis B virus (HBV) capsid inhibitors. *J. Med. Chem.* **2017**, *60*, 3352–3371.
- (22) Wang, X. Y.; Wei, Z. M.; Wu, G. Y.; Wang, J. H.; Zhang, Y. J.; Li, J.; Zhang, H. H.; Xie, X. W.; Wang, X.; Wang, Z. H.; Wei, L.; Wang, Y.; Chen, H. S. In vitro inhibition of HBV replication by a novel compound, GLS4, and its efficacy against adefovir-dipivoxil-resistant HBV mutations. *Antiviral Ther.* **2012**, *17*, 793–803.
- (23) Zhou, X.; Gao, Z. W.; Meng, J.; Chen, X. Y.; Zhong, D. F. Effects of ketoconazole and rifampicin on the pharmacokinetics of GLS4, a novel anti-hepatitis B virus compound, in dogs. *Acta Pharmacol. Sin.* **2013**, *34*, 1420–1426.
- (24) Wu, G.; Liu, B.; Zhang, Y.; Li, J.; Arzumanyan, A.; Clayton, M. M.; Schinazi, R. F.; Wang, Z.; Goldmann, S.; Ren, Q.; Zhang, F.; Feitelson, M. A. Preclinical characterization of GLS4, an inhibitor of hepatitis B virus core particle assembly. *Antimicrob. Agents Chemother.* **2013**, *57*, 5344–5354.
- (25) Klumpp, K.; Lam, A. M.; Lukacs, C.; Vogel, R.; Ren, S.; Espiritu, C.; Baydo, R.; Atkins, K.; Abendroth, J.; Liao, G.; Efimov, A.; Hartman, G.; Flores, O. A. High-resolution crystal structure of a hepatitis B virus replication inhibitor bound to the viral core protein. *Proc. Natl. Acad. Sci. U. S. A.* **2015**, *112*, 15196–15201.
- (26) Abbott, G. W.; Sesti, F.; Splawski, I.; Buck, M. E.; Lehmann, M. H.; Timothy, K. W.; Keating, M. T.; Goldstein, S. A. MiRP1 forms IKr potassium channels with hERG and is associated with cardiac arrhythmia. *Cell* **1999**, *97*, 175–187.
- (27) Fermini, B.; Fossa, A. A. The impact of drug-induced QT interval prolongation on drug discovery and development. *Nat. Rev. Drug Discovery* **2003**, *2*, 439–447.
- (28) Jamieson, C.; Moir, E. M.; Rankovic, Z.; Wishart, G. Medicinal chemistry of hERG optimizations: highlights and hang-ups. *J. Med. Chem.* **2006**, *49*, 5029–5046.
- (29) Ren, Q.; Liu, X.; Luo, Z.; Li, J.; Wang, C.; Goldmann, S.; Zhang, J.; Zhang, Y. Discovery of hepatitis B virus capsid assembly inhibitors leading to a heteroaryldihydropyrimidine based clinical candidate (GLS4). *Bioorg. Med. Chem.* **2017**, *25*, 1042–1056.
- (30) Bourne, C. R.; Finn, M. G.; Zlotnick, A. Global structural changes in hepatitis B virus capsids induced by the assembly effector HAP1. *J. Virol* **2006**, *80*, 11055–11061.
- (31) Berke, J. M.; Verbinnen, T.; Tan, Y.; Dehertogh, P.; Vergauwen, K.; Vanduyck, K.; Lenz, O. The HBV capsid assembly modulator JNJ-379 is a potent inhibitor of viral replication across full length genotype A-H clinical isolates in vitro. Presented at the AASLD Liver Meeting, Washington, DC, Oct 20–24, 2017.
- (32) Baell, J. B.; Holloway, G. A. New substructure filters for removal of pan assay interference compounds (PAINS) from screening libraries and for their exclusion in bioassays. *J. Med. Chem.* **2010**, *53*, 2719–2740.